

AD-A034 029

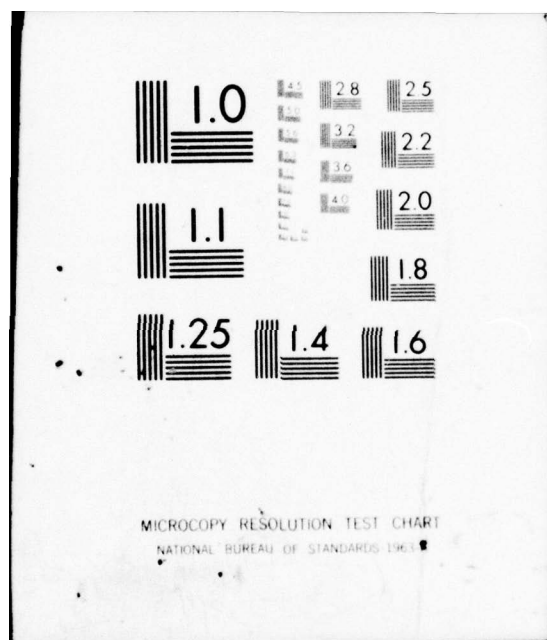
AIR FORCE INST OF TECH WRIGHT-PATTERSON AFB OHIO SCH--ETC F/6 20/12
DEPTH-RESOLVED CATHODOLUMINESCENCE ON THE EFFECTS OF CD IMPLANT--ETC(U)
DEC 76 J D DUMOULIN
SEP/PH/76-2

UNCLASSIFIED

NL

1 OF 1
AD
A034 029





ADA034029

⑨ Master's thesis,

⑥ DEPTH-RESOLVED
CATHODOLUMINESCENCE ON THE
EFFECTS OF Cd IMPLANTATION
AND ANNEALING IN
GALLIUM ARSENIDE.

THESIS

⑭ GEP/PH/76-2

⑩ Joseph D. Dumoulin
Captain USAF

⑪ Dec 76

⑫ 75p.

Approved for public release; distribution unlimited

ACCESSION BY	
DTIC	Write Section <input checked="" type="checkbox"/>
DDC	Ref Section <input type="checkbox"/>
UNANNOUNCED	<input type="checkbox"/>
JUSTIFICATION	
BY	
DISTRIBUTION/AVAILABILITY CODES	
Dist.	AVAIL. and/or SPECIAL

012225

DEPTH-RESOLVED CATHODOLUMINESCENCE
ON THE EFFECTS OF Cd IMPLANTATION
AND ANNEALING IN GALLIUM ARSENIDE

THESIS

Presented to the Faculty of the School of Engineering
of the Air Force Institute of Technology
Air University
in Partial Fulfillment of the
Requirements for the Degree of
Master of Science

by

Joseph D. Dumoulin

Captain USAF

Graduate Engineering Physics

December 1976

Approved for public release; distribution unlimited

Preface

This thesis has been sponsored by the Air Force Avionics Laboratory/DHR. I would like to thank this organization for providing the ion implanted samples, the liquid helium, and the annealing facilities used in the experiment.

In completing this thesis there were many people whose help I needed, and received. I am especially grateful to my advisor, Dr. Robert L. Hengehold, who I will remember most for showing me the two qualities that are of greatest importance to an experimentalist: unbounded optimism, and patience. Major Bruce J. Pierce first interested me in this topic and the help he gave me to become familiar with the cathodoluminescence system was an excellent beginning for this project. I am also grateful for the timely and skilled assistance given to me by George Gergal, Jim Miskimen and Ron Gabriel of the AFIT physics laboratory staff.

Joseph D. Dumoulin

Contents

	Page
Preface	ii
List of Figures	v
List of Tables	vi
Abstract.	vii
I. Introduction	1
II. Theory	4
Radiative Recombination	4
Simple Center.	4
Complex Center.	6
Ion Implantation	7
Annealing	9
Diffusion.	10
Electron Beam Penetration	12
III. Experiment.	16
Cathodoluminescence System	16
Luminescence Detection	18
Signal Processing.	19
Procedure	20
Optical Alignment.	20
Data Recording	21
Sample Annealing/Cap Removal	22
IV. Results and Discussion	25
Peak Energies	26
Cadmium Implanted GaAs with Fluence = 10^{12} ion/cm ²	26
Cadmium Implanted GaAs with Fluence = 10^{14} ion/cm ²	31
Cadmium Implanted GaAs with Fluence = 10^{15} ion/cm ²	31

	Page
Cadmium Implanted GaAs with Fluence = 10^{16} ion/cm ²	34
Unimplanted GaAs	36
Damage Layer	38
Cadmium Implanted GaAs with Fluence = 10^{12} ion/cm ²	40
Cadmium Implanted GaAs with Fluence = 10^{14} ion/cm ²	43
Cadmium Implanted GaAs with Fluence = 10^{15} ion/cm ²	46
Cadmium Implanted GaAs with Fluence = 10^{16} ion/cm ²	49
Unimplanted GaAs	51
Annealing Effects	53
Cadmium Implanted GaAs with Fluence = 10^{12} ion/cm ²	55
Cadmium Implanted GaAs with Fluence = 10^{14} ion/cm ²	56
Cadmium Implanted GaAs with Fluence = 10^{15} ion/cm ²	57
V. Conclusions and Recommendations	58
Conclusions	58
Recommendations	59
Bibliography	61
Vita	65

List of Figures

<u>Figure</u>		<u>Page</u>
1	Cadmium Implanted GaAs Profile (Ref 31:1577)	10
2	Estimated Electron Excitation Profiles in GaAs (Ref 4:12)	13
3	Cathodoluminescence System Schematic	17
4	Annealing System Schematic	23
5	Typical Spectra of Samples 8 and 8AA at 10°K	27
6	Typical Spectra of Sample 8A at 10°K and 80°K . . .	28
7	Typical Spectra of Sample 4 at 10°K and Sample 4A at 10°K and 80°K	32
8	Typical Spectra of Samples 6, 6A and 7 at 10°K . . .	33
9	Depth Resolved Spectra of Sample 6A at 10°K. . . .	35
10	Typical Spectra of Samples 11 and 11AC at 10°K . . .	37
11	Damage Layer Spectra of Sample 8 at 10°K	41
12	Damage Layer Spectra of Sample 8AA at 10°K	42
13	Damage Layer Spectra of Samples 4 and 4A at 10°K .	44
14	Damage Layer Spectra of Sample 6 at 10°K	47
15	Damage Layer Spectra of Sample 6A at 10°K	48
16	Damage Layer Spectrum of Sample 7 at 10°K	50
17	Near Surface Spectra of Sample 11AC at 10°K.	52

List of Tables

<u>Table</u>		<u>Page</u>
I	Sample Labeling System	25
II	Damage Layer Depths--All Samples, 10°K	39
III	Intensities of Selected Peaks.	54

Abstract

Ten samples of GaAs were examined by depth-resolved cathodoluminescence at temperatures of 10°K and 80°K. Electron beam energies from 1.0 KV to 25KV were used. Both cold and hot, 135KV, Cd-implanted GaAs samples with Si₃N₄ caps were studied. A sample of the n-type GaAs substrate was used as a control. Spectra were obtained showing the ion implantation damage layers. The unannealed samples damage layer boundaries were calculated at 0.01 μm, 0.24 μm, 0.37 μm, and 0.61 μm for fluences of 10¹² ion/cm², 10¹⁴ ion/cm², 10¹⁵ ion/cm², and 10¹⁶ ion/cm² respectively. For fluences ≥ 10¹⁴ ion/cm² an 800°C, 15 minute anneal in flowing argon gas was not sufficient to completely remove the damage layer. An emission peak at 1.488eV changed in energy by only 0.001eV between 10°K and 80°K, and was assigned to a donor-Cd acceptor recombination. A peak approximately 0.010eV above the band gap energy was observed in many of the implanted samples. Peaks at 1.46eV, 1.41eV, 1.39eV, and 1.35eV increased in intensity upon annealing and were assigned to vacancies, which were enhanced during annealing. The major conclusion reached was that depth-resolved cathodoluminescence was an excellent non-destructive method of sharply defining damage layers produced by ion implantation. Another conclusion was that LSS theory does not predict the correct Cd concentration in unannealed GaAs at the damage layer boundary for fluences ≥ 10¹⁴ ion/cm².

I. Introduction

The United States Air Force uses devices which must operate in high temperature environments, where presently available semiconductors do not perform well. Further, new device applications, such as microwave devices, are waiting upon the development of semiconductors which possess the desired electrical properties. With proper doping, the intentional addition of impurity ions to the lattice of a semiconductor, the semiconductor gallium arsenide (GaAs) should have the electrical properties necessary for excellent operation in the areas mentioned above.

Gallium arsenide is an intermetallic compound formed from a group III element, gallium, and a group V element, arsenic. It crystallizes in the zinc blende structure and has physical properties which are very similar to those of the covalent group IV elements, such as germanium and silicon. Most of the differences between the group IV covalent elements and III-V semiconductors, like GaAs, are due to the latter's slightly ionic character. The electrical properties, such as high electron mobility, have made them very useful in many technical applications (Ref 27:371-372). But, the promise that GaAs shows for use in microwave devices and high temperature environments is based upon the ability to provide the necessary dopant

concentrations in the "pure" crystal.

The Air Force Avionics Laboratory, Wright-Patterson Air Force Base, Ohio, is presently studying ion implantation as a doping method in GaAs. Ion implantation has been successfully used to provide the impurity concentration profiles necessary in silicon semiconductors, but not enough is known about its effects in GaAs to make it a useful doping method of this semiconductor at the present time. Additional information is needed in the areas of impurity concentration profiles, lattice damage, annealing effects, electrical activity, and lattice structure after implantation and damage removal.

The purpose of this study was to examine the damage done to the GaAs lattice by Cd implantation, to determine the effects of annealing on this damage, and to investigate the lattice structure with respect to the Cd ions lattice positions and the presence of vacancies and native defects. The experimental laboratory technique of depth-resolved cathodoluminescence was used to study the luminescence from different depths in the GaAs samples. Luminescence is that phenomena in which a portion of energy absorbed by matter is emitted in the form of visible radiation. When the excitation source used to produce luminescence is a beam of energetic electrons the process is called cathodoluminescence. In depth-resolved cathodoluminescence the layer of the crystal from which luminescence is produced is controlled by the accelerating potential of the electrons used for bombardment. This technique has already been used to study GaAs (Ref 4:28) and ZnO

(Ref 30).

Four Cd-implanted Si_3N_4 capped GaAs samples at fluences from 10^{12} ion/cm² to 10^{16} ion/cm² and one unimplanted sample of the substrate material were provided by the Air Force Avionics Laboratory. Three of the implanted samples were annealed at 800°C for 15 minutes in flowing argon gas. The 10^{12} ion/cm² fluence sample was annealed again for an additional 15 minutes at 800°C. Comparing the results from the study of the luminescence of these samples to electrical measurements obtained from Hall-effect and differential capacitance studies will help the Air Force Avionics Laboratory to understand the damage effects of ion implantation, the effects of annealing on this damage, and the lattice structure of ion-implanted GaAs. In addition it is hoped that this organization will be able to determine a relationship between electrical activity and optical activity in GaAs by performing electrical measurements on those samples examined in this study.

Chapter II contains the theory necessary to support the discussion of the experimental results. In Chapter III the experimental apparatus and arrangement are described and the important experimental procedures are presented. Chapter IV is a discussion of the experimental results, and finally in Chapter V some conclusions and recommendations are listed.

II. Theory

In this chapter the theory will be presented which is necessary for an adequate understanding of the discussion of results and of the conclusions reached. Some of the material has been covered in detail in prior thesis work and will only be referenced here. The major topics appearing in this section are the following: radiative recombination, ion implantation, annealing, diffusion, and electron beam penetration.

Radiative Recombination

When a material such as GaAs is excited with a beam of electrons, or some other excitation source, luminescence results. This luminescence is created by the radiative recombination of electron-hole pairs produced during the excitation. The radiative recombination can involve simple or complex centers.

Simple Center. A simple center is an impurity sitting on a lattice site which contributes one additional carrier to the binding. The activation energy of a simple center is close to that calculated from the hydrogenic model. The four main simple center radiative recombinations are: valence band-conduction band, exciton, free-bound, and bound-bound. Boulet (Ref 4:4-8) has presented a detailed explanation of each of these recombinations and only the bound-bound one will be discussed here.

The recombination energy of an electron bound to a donor impurity and a hole bound to an acceptor impurity can be described by the following equation (Ref 4:7, 13:744):

$$E_B = E_G - (E_A + E_D) + e^2/kR \quad (1)$$

where

E_B = energy of bound-bound transition

E_G = band gap energy

E_A = acceptor binding energy

E_D = donor binding energy

e = electron charge

k = static dielectric constant

R = separation between donor and acceptor sites

The band gap energy is a function of temperature and decreases approximately 10 meV between liquid helium and liquid nitrogen temperatures (Ref 32:770). The e^2/kR term is also a function of temperature but it increases as temperature increases. As the temperature increases acceptors are thermally released from donor sites and move to more favorable positions for recombination, positions for which R is smaller (Ref 15:792, 22:843). This causes the energy peak to shift to higher energy, which offsets the shift to lower energy caused by band gap energy decrease. Therefore, as temperature is increased a peak due to bound-bound recombination will shift toward lower energy by a smaller amount than the band gap shift. It should be

pointed out, that a peak due to a free-bound recombination also does not shift toward lower energy as much as the band gap does with increasing temperature. However the difference in the shift is the amount of thermal energy the free particle has, about 3.4 meV at 80°K using $KT/2$ to represent the thermal energy (Ref 4:6). So it is possible to distinguish between bound-bound and free-bound energy peaks by the shift of the peak with temperature.

Complex Center. A complex center involves a deep level impurity or a vacancy complex which has an activation energy that does not follow the hydrogenic model. Their luminescence levels are low in energy and broad in extent. In p-type GaAs deep-level luminescence commonly occurs at 1.42eV, 1.35eV, and 1.37eV. The literature shows no firm agreement as to whether these peaks are caused by impurities or vacancy complexes. The 1.41eV peak will be used to illustrate this disagreement. Studies in which GaAs crystals were doped with Mn convinced some researchers that the 1.41eV peak was due to an Mn impurity; because this doping produced a new peak at 1.41eV, or greatly enhanced one that was already there (Ref 23:54, 24:3062). Studies in which undoped GaAs samples are annealed under different conditions have indicated that the 1.41eV peak is due to vacancies (Ref 8:144, 12). By annealing boat grown n-type GaAs in sealed quartz ampoules under different temperatures and different As pressures Chang et al. were able to show that the 1.4eV peak could be suppressed with increased As pressure during annealing (Ref 7). This

indicates that the peak is due to As vacancies since at the higher As overpressure fewer As atoms would be expected to diffuse out of the GaAs material. In general, for almost all complex peaks doping studies have indicated that the dopant is responsible for the energy peaks while annealing studies have indicated that vacancies are responsible.

Ion Implantation

Ion implantation is the process of injecting high energy impurity ions into the substrate of a semiconductor. This process damages the semiconductor in two ways. First, ions of the substrate are sputtered from the surface under this bombardment process. Second and more important, is the 'tearing' of the lattice structure of the semiconductor by the high energy ions as they collide with the lattice atoms, removing them from their orderly arrangement. This damage must be removed before electrical activity can be obtained from the semiconductor, and the advantages of ion implantation over other doping methods make it worthwhile to do this. These advantages include the ability to introduce precise concentrations of almost any impurity desired at any depth desired and the ability to avoid high temperature problems that are associated with the diffusion method of impurity doping (Ref 4:2). Before discussing the means of ion implantation damage removal, the way in which ions are slowed by the lattice material must be covered.

The relationship between energy loss and range distribution for ion implantation is governed by two major factors: the interaction of the ions with the electrons of the substrate and the collisions of the ions with the nuclei of the target atoms. The theory of Lindhard, Scharff, and Schiott (LSS theory) which takes these effects into account, while neglecting quantum effects, can be used to predict the projected range (R_p) of the ions into the target material (Ref 17:298). The projected range is the depth at which the ions are deposited in the material, rather than the total path length of the ions. The LSS implantation profile, concentration of ions versus depth of ions in the material, can be calculated using the following equation (Ref 18):

$$N(X) = \frac{\phi}{\sqrt{2\pi} \Delta R_p} \text{EXP} \left[-\frac{(X-R_p)^2}{2(\Delta R_p)^2} \right] \quad (2)$$

where

$N(X)$ = ion concentration (cm^{-3})

ϕ = fluence (ion/cm^2)

X = distance into substrate

ΔR_p = projected range standard deviation

In calculating concentrations in this study values for R_p and ΔR_p were obtained from the tabular listing of LSS range statistics of Cd-implants in GaAs presented by Gibbons et al (Ref 18). The ion implantation of the samples used in this experiment was done through a 300 Å Si_3N_4 cap to protect the sample surface from loss due to sputtering. Therefore, it is also necessary to include the Si_3N_4 cap

thickness when calculating the LSS profile. It has been assumed that the values for R_p and ΔR_p used for Cd-ion penetration in GaAs can also be used for the penetration of the Si_3N_4 cap, since the density of the two materials is not greatly different, 5.90 g/cm^3 and 3.44 g/cm^3 respectively. After the ion concentration has been calculated, using equation (2), with a specified X value the depth of the cap is subtracted from the X value to give the depth in the GaAs crystal at which this ion concentration is present. This procedure is necessary in order to correlate ion concentration with the depth of electron penetration into the GaAs samples.

Annealing

The heat treatment, or annealing of ion-implanted samples is necessary for two reasons. First, it helps to reduce the damage caused by the energetic ions as they tear through the lattice. Second, annealing moves the majority of ions to substitutional lattice sites enabling them to become electrically active. In order for annealing to be effective on ion-implanted GaAs it has been shown that temperatures between 800°C and 900°C are necessary (Ref 1:146, 9:568, 23:55, 31:1575). Unfortunately, at temperatures near 600°C the GaAs surface begins a significant decomposition; and it therefore is necessary to protect the surface with an Si_3N_4 or SiO_2 cap. The use of a cap also helps to prevent outdiffusion of Ga and As which, if allowed, produces unwanted vacancies in the lattice structure (Ref 9:568). However, it has been shown that SiO_2 caps enhance outdiffusion of As (Ref 10:1423).

Outdiffusion can be reduced by annealing in sealed ampoules with overpressure of Ga and/or As (Ref 8:144). But this method has been shown to introduce impurities into the GaAs, such as Cu, when the anneal is carried out in a sealed quartz ampoule (Ref 11:317). Annealing in flowing hydrogen or argon gas avoids contamination from the ampoule and the cap helps to prevent the gas and other impurities from entering the crystal. However outdiffusion cannot be prevented by Ga or As overpressure.

Diffusion

Annealing, besides causing the outdiffusion of Ga and As, causes the implanted ions to diffuse far into the GaAs crystal. This diffusion has been substantiated by many experiments and a graph presented in one such study is shown in Fig. 1 (Ref 31:1577).

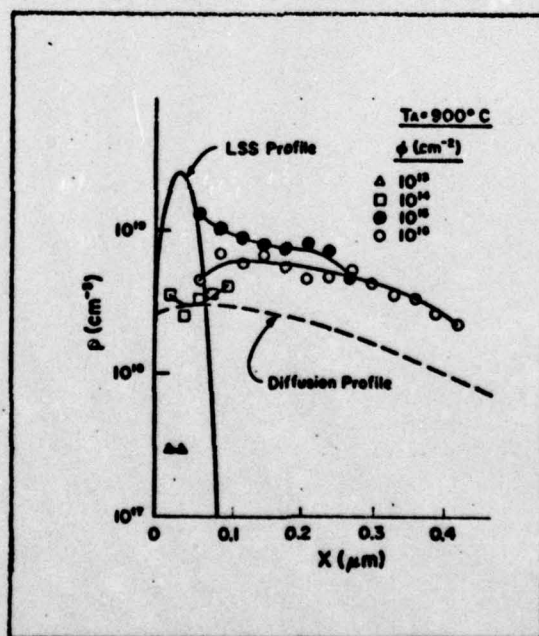


Fig. 1. Cadmium Implanted GaAs Profile (Ref 31:1577)

The diffusion profile and LSS profile are shown for a fluence of 10^{14} ion /cm². Measured data for different fluences is also shown. The extent of the ion diffusion for a 900°C anneal is illustrated very well in this figure. The diffusion profile is based upon the diffused Gaussian distribution which can be calculated from the following equation (Ref 23:55):

$$N(X) = \frac{\phi}{[2\pi(\Delta R_p^2 + 2Dt)]^{1/2}} \text{EXP} \left[-\frac{(X - R_p)^2}{2(\Delta R_p)^2 + 4Dt} \right] \quad (3)$$

where

D = diffusion coefficient (cm²sec⁻¹)

t = time of anneal

The diffusion coefficient can be calculated as a function of temperature from the following equation:

$$D = D_0 \text{EXP} (E/kT) \quad (4)$$

where

E = average activation energy of Cd in GaAs

The values used in this equation for calculating the diffusion curve in Fig. 1 are: $D_0 = 1.3 \times 10^{-3}$ cm²sec⁻¹ and $E = 2.2$ eV (Ref 16:727).

There are two possible explanations given for the way in which p-type impurities, such as Cd or Zn, diffuse through the III-V lattice. Substitutional diffusion requires the impurity ion to move through the lattice by jumping from one vacancy to another. It forms the basis for equation (3). Paired vacancies are necessary in GaAs since the nearest neighbor for each gallium atom is an arsenic atom. This

requirement for paired vacancies is the problem with the substitutional diffusion theory. It is believed that enhanced vacancy density occurs in only arsenic sites for heavy p-doping. Therefore, a substitutional Cd/Zn ion would have to move interstitially in order to get from one arsenic vacancy to another. In the interstitial substitutional diffusion model the Cd/Zn ion goes into the lattice interstitially, acting as a donor. It is stable and diffuses interstitially through the lattice very rapidly with heating (Ref 25:127-128).

Electron Beam Penetration

Electron penetration into GaAs, ZnO, and other luminescent crystals at a 45° angle to the surface has been well discussed and extensively used by a number of different researchers (Ref 4:9-12, 28, 30:645). Fig. 2 on the following page shows the electron excitation profile in GaAs at selected beam energies (Ref 4:12). It is important to note that the electrons give up their energy to the GaAs crystal over a range of depths, and that the greatest amount of energy is deposited much closer to the surface than at the maximum electron penetration for that energy. Therefore, any luminescence caused by a 15 KV electron, for example, is coming from an area of the crystal that extends from the surface to approximately 1.4 μm below the surface.

In this experiment it has been necessary to calculate the depth to which the damage layer created by ion implantation extends. It therefore is necessary to calculate the maximum extent of electron

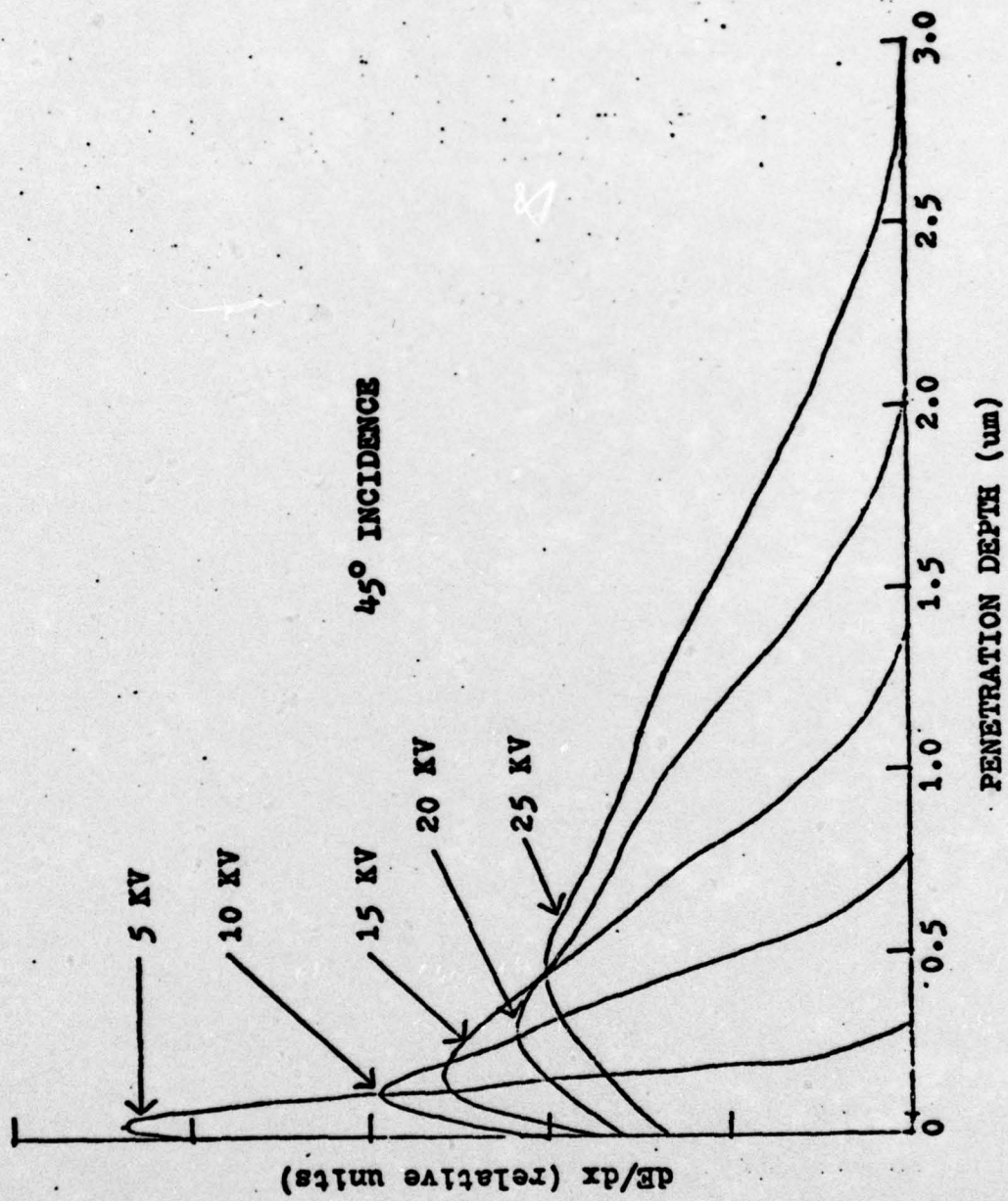


Fig. 2. Estimated Electron Excitation Profiles in GaAs (Ref 4:12)

penetration into the GaAs crystal. To do this an empirical formula developed by Martinelli and Wang has been used (Ref 26:3351).

$$R = aE_p^b \quad (5)$$

where

R = electron range penetration (μm)

E_p = electron energy (KV)

a, b = material constants determined to be $0.027 \pm 0.003 \mu\text{m}$
and 1.46 ± 0.05 respectively

To develop this formula GaAs films in the thickness range 0.19-1.5 μm were radiated with electrons of a given initial energy. When these electrons emerged from the exit surface of a film with an energy of several hundred eV they were considered to have a penetration depth equal to the film thickness. The results of this formula compare very well with the data in Fig. 2, which was obtained from the universal electron stopping curve (Ref 29:28). Since in this experiment the cathodoluminescence was obtained with the Si_3N_4 cap still present, the electron energy needed to penetrate the 300 \AA cap had to be calculated. From the universal electron stopping curve values for electron range penetration in mg/cm^2 can be found for a given electron energy (Ref 29:174). By dividing these electron range penetration values by the density of the Si_3N_4 cap the electron range penetration in Si_3N_4 can be calculated for the corresponding electron energy. Using a density value of $3.44 \times 10^{-3} \text{ mg}/\text{cm}^3$ for Si_3N_4 (Ref 6:711-712) it was found that 1.75 KV electrons were needed to penetrate a 308 \AA Si_3N_4 cap.

It was later found experimentally that the energy needed was closer to 1.5 KV. By subtracting the 1.5 KV energy from the power supply voltage meter reading and then using equation (5) the maximum depth at which luminescence was being excited in the GaAs crystal was calculated.

III. Experiment

The cathodoluminescence system used in this experiment was very similar to that used by Boyd, and his thesis should be referenced by those who wish additional information on the equipment and system description (Ref 5:16-34). In order to study the damage layer produced during ion implantation and the affects of annealing on the implanted samples it was necessary to use electron beam energies (E_B) extending from 1KV to 25KV with beam currents (I_B) extending from 0.1 μ a to 3.4 μ a. This chapter examines the cathodoluminescence system and the procedures used in this experiment.

Cathodoluminescence System

A simplified schematic of the cathodoluminescence system is shown in Fig. 3 on the following page. The system operated in the following way. A Superior Electronics 5AZP4 electron gun, located vertically below the sample chamber, provided electrons for sample bombardment. The electrons were accelerated by the potential provided by a Universal Voltronics BAC 50-16 high voltage supply. An Andonian Associates Model MHD-3L-30N liquid helium dewar was used to cool the samples. A GaAs thermometer registered sample block temperatures of 80°K using liquid nitrogen and 10°K using liquid helium. A vacuum from 4×10^{-6} torr to 2×10^{-7} torr was maintained

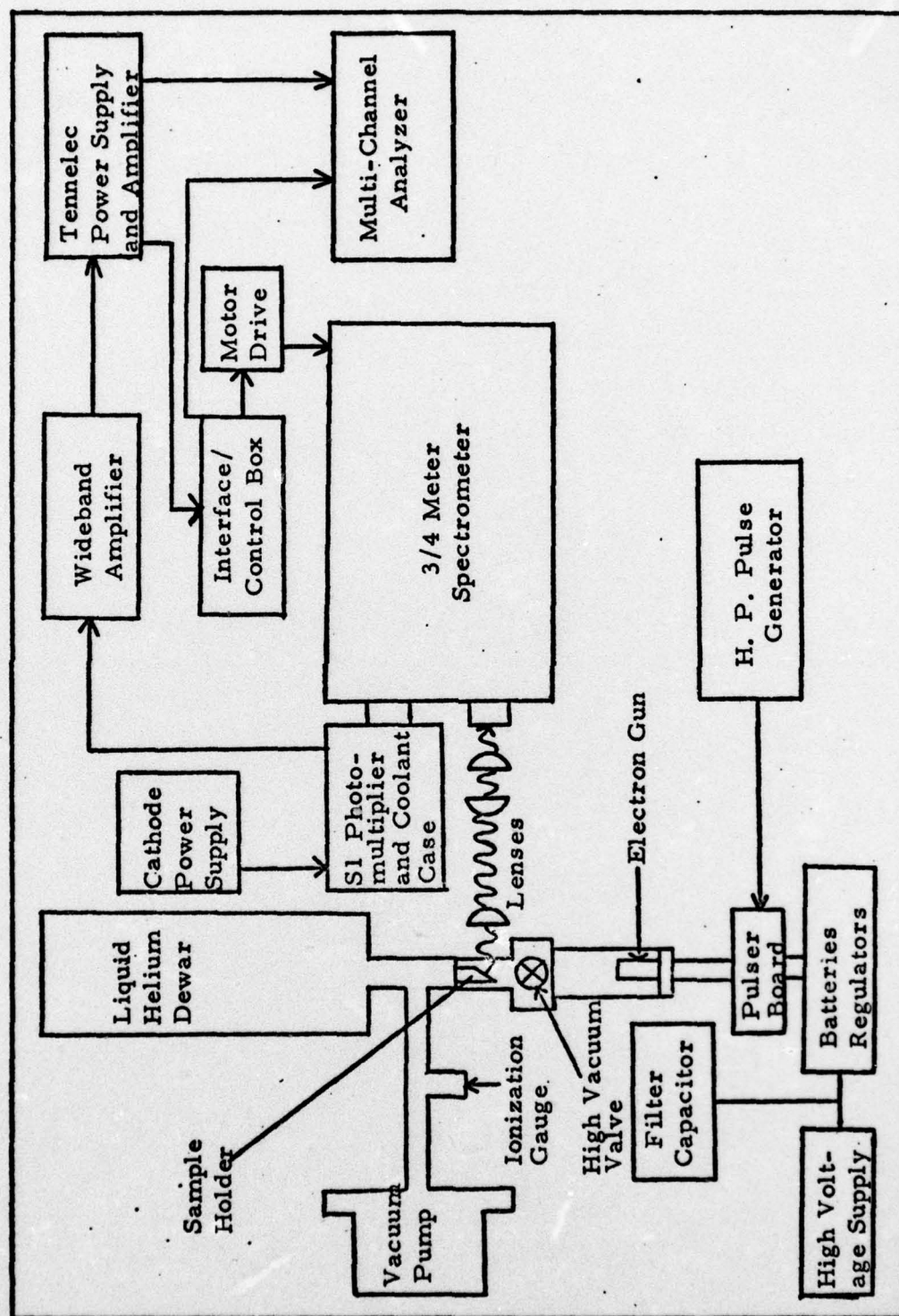


Fig. 3. Cathodoluminescence System Schematic

in the dewar, sample chamber, and electron gun chamber by use of a Welch Scientific Company Series 3102D turbo-molecular pump. The luminescence detection and signal processing used in this experiment are described in detail in the remainder of this section.

Luminescence Detection. After passing through a quartz window of the sample chamber, the sample luminescence was focused onto the spectrometer slit by three plano convex quartz lenses mounted on an Ealing 50-centimeter optical bench. Each lens mounting had three degrees of freedom, making precise focusing possible. The lens closest to the samples had a focal length of 10 centimeters, and was positioned at approximately this distance from the samples. The other two lenses were in the same mount, with a fixed separation of 8 centimeters; and they were positioned near the spectrometer slit. A Spectraccoat Varipass number 650 filter of set 6193 was also placed in this mount to reduce the amount of light from the electron gun reaching the spectrometer slit. The filter transmits 90% of the incident radiation at or above a wavelength of 6500 \AA while being essentially opaque to those wavelengths below 6500 \AA . The lens closest to the spectrometer slit had a 6.5 centimeter focal length, while the focal length of the other lens was 25 centimeters. A SPEX Model 1702 3/4-meter Czerny-Turner spectrometer was used to examine the luminescence. A SPEX Model 1752-3 motor drive unit provided external stepping signals to the spectrometer. The motor drive was controlled by the interface/control box designed and constructed by G. Gergal and

described in great detail by Boyd (Ref 5:27-29). One additional spectrometer step per channel setting at 25 was added to this device which enabled a 1600 \AA scan to be completed in approximately half the minimum time obtainable before. The signal intensity reduction was not critical, and the amount of data collected for the available liquid helium was nearly doubled. An RCA C70007A photomultiplier tube with S1 response was used to detect the spectrometer output signal. The tube was cooled to -50°C by use of a Model TE-114 cooling chamber manufactured by Products for Research. The cathode bias of the tube was supplied by a Model 404M Fluke power supply.

Signal Processing. The signal processing scheme used in this experiment was designed to permit photon counting to be employed in the recording of the luminescence spectra. The current from the photomultiplier tube anode was supplied to a Keithley Instrument 104 wideband amplifier. The output from this device entered a Tennelec TC907B power supply/TC200 amplifier. This arrangement was used to amplify and process the signal so that the correct number of properly shaped pulses corresponding to the true signal strength would be passed to a Hewlett Packard Model 5400 multi-channel analyzer (1024 channels) for counting. From the Tennelec amplifier the signal was passed to both the multi-channel analyzer and the interface/control box. The interface/control box stepped the spectrometer and the channels of the multi-channel analyzer in the desired ratio (Ref 5:31-32).

Procedure

The procedures described in this section are: optical alignment, data recording, and sample annealing/cap removal.

Optical Alignment. A set of 4 samples were mounted on the sample block located at the end of the cold finger of the helium dewar. The method of optical alignment was basically the same whether it was the first alignment after these samples were changed or when one wanted to switch from one sample to another. Before samples were changed the position of the lenses and the sample position last observed was recorded. Once the new sample set was in place the electron beam was directed at the sample occupying the same position as the sample last observed. This insured that except for minor adjustments the lenses were aligned properly. The spectrometer was set at a wavelength where a strong peak was expected in the sample luminescence. At liquid nitrogen temperatures this was the 1.355eV peak, while at liquid helium temperatures the 1.490eV peak was used. The lens mounts were adjusted until the signal observed on the multi-channel analyzer oscilloscope was a maximum. The alignment procedure when switching from one sample to another was similar. The position of the new sample with respect to the one just observed determined the rough settings of the horizontal and vertical mount controls of the lens closest to the sample block. The other lenses were never adjusted until the maximum signal was obtained using these two controls. In all cases, the alignment of a sample was done at beam voltages from 15 to 25 KV,

which gave the strongest signal possible.

Data Recording. Once a sample had been aligned the lenses were not adjusted again until a new sample was examined. Therefore, for each data run on a sample usually only the beam voltage, beam current, and slitwidth were adjusted. Because the relative intensities of the spectra at different electron beam voltages and for different samples were to be compared, slitwidth and beam current was varied as little as possible. Unfortunately, the beam current had to be increased from the nominal 0.1 μ amp used at 15 KV to 2 μ amp at 5 KV because the luminescence was much weaker at the lower beam voltages and detection became difficult. The slitwidth was also increased from 0.5 millimeters to 1 millimeter respectively. Also, because of the necessity to change interface/control box settings near the middle of data collection some spectral intensities of luminescence spectra taken with identical E_B , I_B , and slitwidth settings could not be compared.

A typical run, after lens adjustment and beam voltage selection, started with the focusing of the electron beam onto the Faraday Cup, which was used to measure the beam current at the sample block. The grid controls of the electron gun were adjusted until the desired current was achieved. The electron beam was then placed on the sample, and the interface/control box settings were checked. The slitwidth was set at 50 microns, the argon lamp turned on, and the spectrometer was set at approximately 7990 \AA . The spectrometer was set to external drive and at 8000 \AA the multi-channel analyzer was turned on.

The calibration lines were recorded by 8020 Å, and the lamp was turned off. The slitwidth was then increased to either .5 millimeters or 1 millimeter. The run was terminated at 9600 Å. The data from memory was displayed on the multi-channel analyzer oscilloscope, a picture taken, and a paper tape of the data was made. This tape was later converted to cards for use in a computer plotting program which generated data graphs, such as those appearing in this thesis. The beam was again moved onto the Faraday cup and any beam current deviation from the starting value was recorded. Another run was ready to begin.

Sample Annealing/Cap Removal. All annealing was performed at the facilities of the Air Force Avionics Laboratory. The annealing system used is shown in Fig. 4 on the following page. All samples were annealed at 800°C in flowing argon gas. The following samples were annealed together for 15 minutes: numbers 8, 4, and 6 (see Table I). Later the 10^{12} ion/cm² fluence sample was again annealed for 15 minutes. A 15 minute anneal was performed on the unimplanted sample with no other samples present. In all anneals the procedure was the same. The sample container, a quartz tube, was cleaned with alcohol and rinsed in distilled water. The holding tube and sample container were placed in the oven support tube and the oven was turned on. The temperature control was adjusted until a temperature of 800°C was registered by the thermocouple. The argon gas pressure at this time was approximately 5 PSI. When the temperature stabilized at

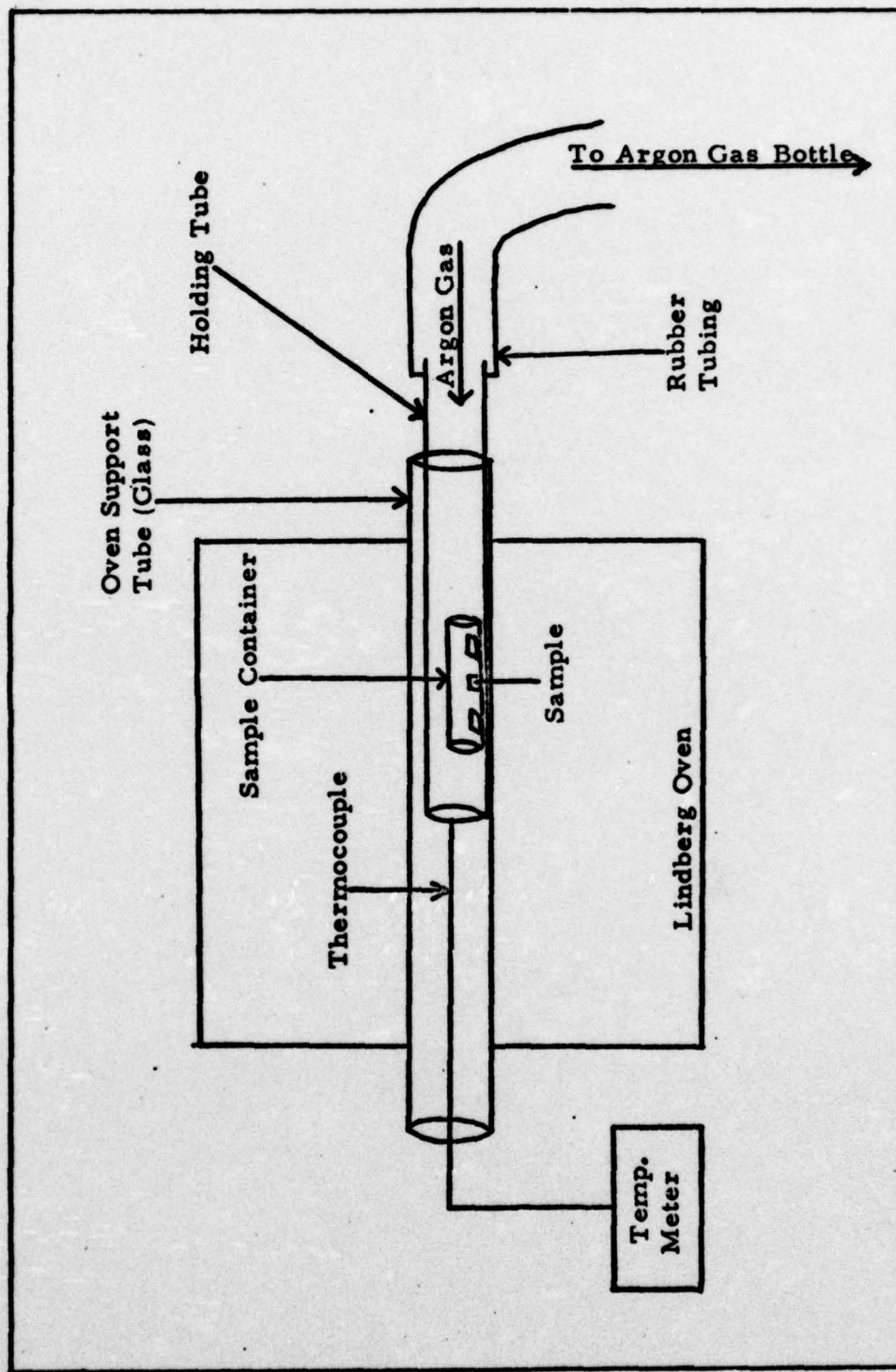


Fig. 4. Annealing System Schematic

800°C, the holding tube was removed from the oven. The sample/ samples were carefully inserted into the hot sample container. The holding tube and sample container were placed back in the oven and the timing began. The temperature initially dropped approximately 20°C and recovered to 800°C about two minutes later. The argon gas pressure during annealing was 10 PSI. When the desired annealing time had elapsed the holding tube was removed from the oven and the sample was left to cool in the sample container.

Only the Si_3N_4 cap of the unimplanted, annealed sample was removed. This was done after the annealing, and consisted of submerging the sample in a 48% HF solution for 10 minutes and then rinsing the sample with distilled water.

IV. Results and Discussion

This chapter contains data obtained from 10 GaAs samples which were examined by depth-resolved cathodoluminescence at liquid helium and liquid nitrogen temperatures. All implantation was done using 135KV Cd ions with a flux of $\approx 1 \mu\text{a}/\text{cm}^2$. Two of the samples were cold implants, i. e. implanted at room temperature, and two of the samples were hot implants, i. e. implanted at 250°C. All annealing was at 800°C in flowing argon gas. The cap was removed from only the unimplanted annealed sample (#11AC). The following table presents the sample conditions and a numbering system to be used for future reference.

Table I
Sample Labeling System

Type	Fluence (ion/cm ²)	Annealing (minutes)	Number	Remarks
Unimplanted	--	--	11	n-type $\approx 10^{16} \text{ cm}^{-3}$ 'as grown material'
Cold	10^{12}	--	8	Samples 8, 4, 6, & 7 were from the same boule as sample 11.
Cold	10^{14}	--	4	
Hot	10^{15}	--	6	
Hot	10^{16}	--	7	
Unimplanted	--	15	11AC	The cap was removed after annealing.
--	10^{12}	15	8A	The unannealed and annealed samples are separate pieces from the same sample.
--	10^{14}	15	4A	
--	10^{15}	15	6A	
--	10^{12}	30	8AA	Sample 8A annealed an additional 15 min.

The data is presented in a manner which illustrates the three major results of this study. They are: peak energies, damage layers, and annealing results.

Peak Energies

All peak energies are considered accurate to within ± 1 meV. This error was primarily due to the fact that each multi-channel analyzer channel contained data over a 1.74 \AA spectrometer scan. Although no peak energies were calculated from the computer plots, these energies were checked and found in agreement with the values calculated from the raw channel number data.

Cadmium Implanted GaAs with Fluence = 10^{12} ion/cm^2 . Typical spectra for samples 8 and 8AA at 10°K and sample 8A at 10°K and 80°K are shown in Fig. 5 and Fig. 6 on the following pages. A peak at 1.53eV appears in the spectra of samples 8 and 8A at 10°K . This energy is above the band gap energy which is near 1.52eV at 21°K (Ref 32:770). This peak does not appear in the unimplanted annealed sample with the cap removed, nor does it appear in many of the ion-implanted samples. Sturge (Ref 32:772) also found a peak at 1.53eV when he placed a glass backing on a GaAs sample. The peak widened and nearly disappeared with polishing. He believed this peak was caused by the strain introduced in the sample during cooling by the different coefficients of expansion for the glass and the GaAs crystal. This strain caused the band gap energy to increase and the valence

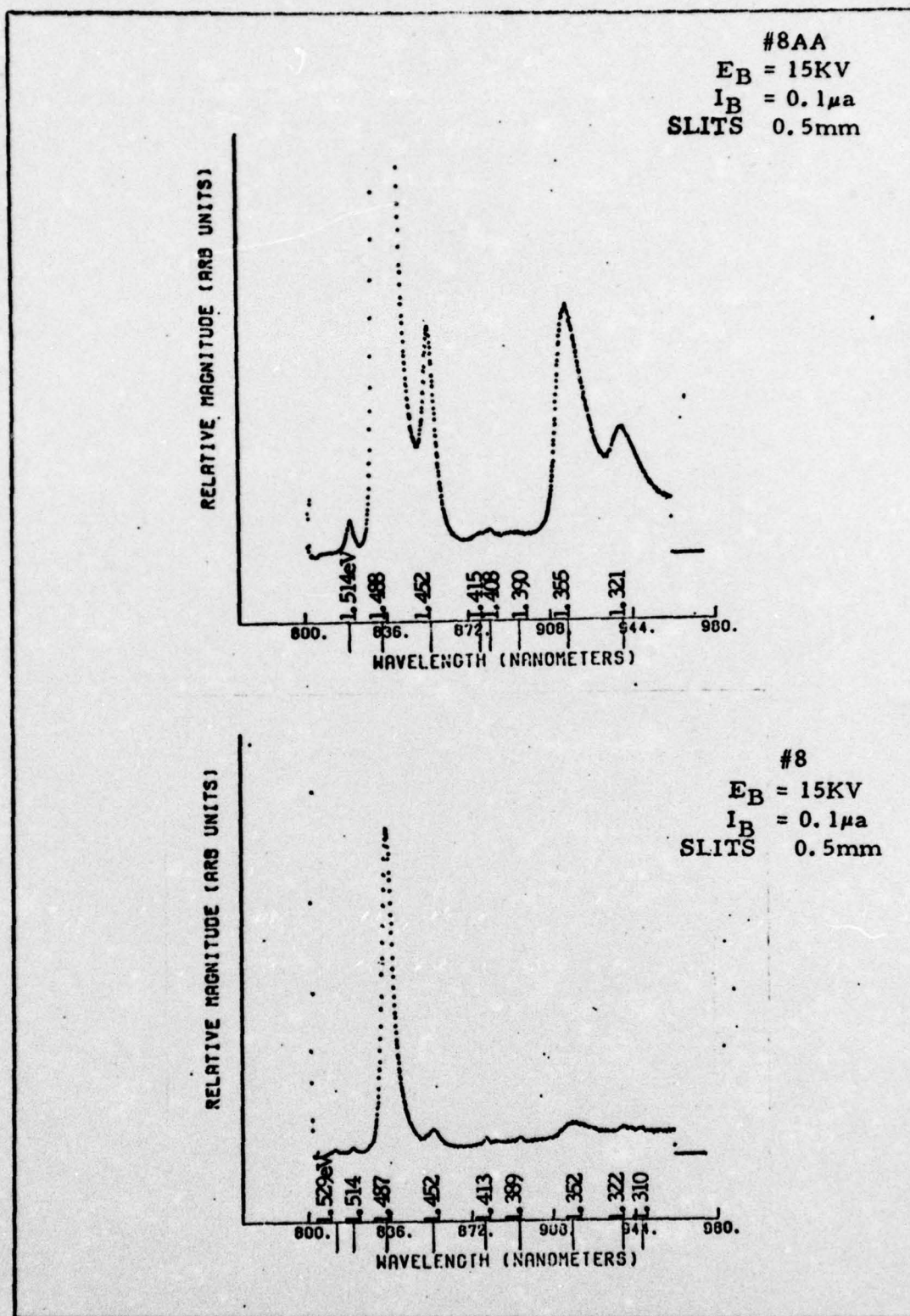


Fig. 5. Typical Spectra of Samples 8 and 8AA at 10°K

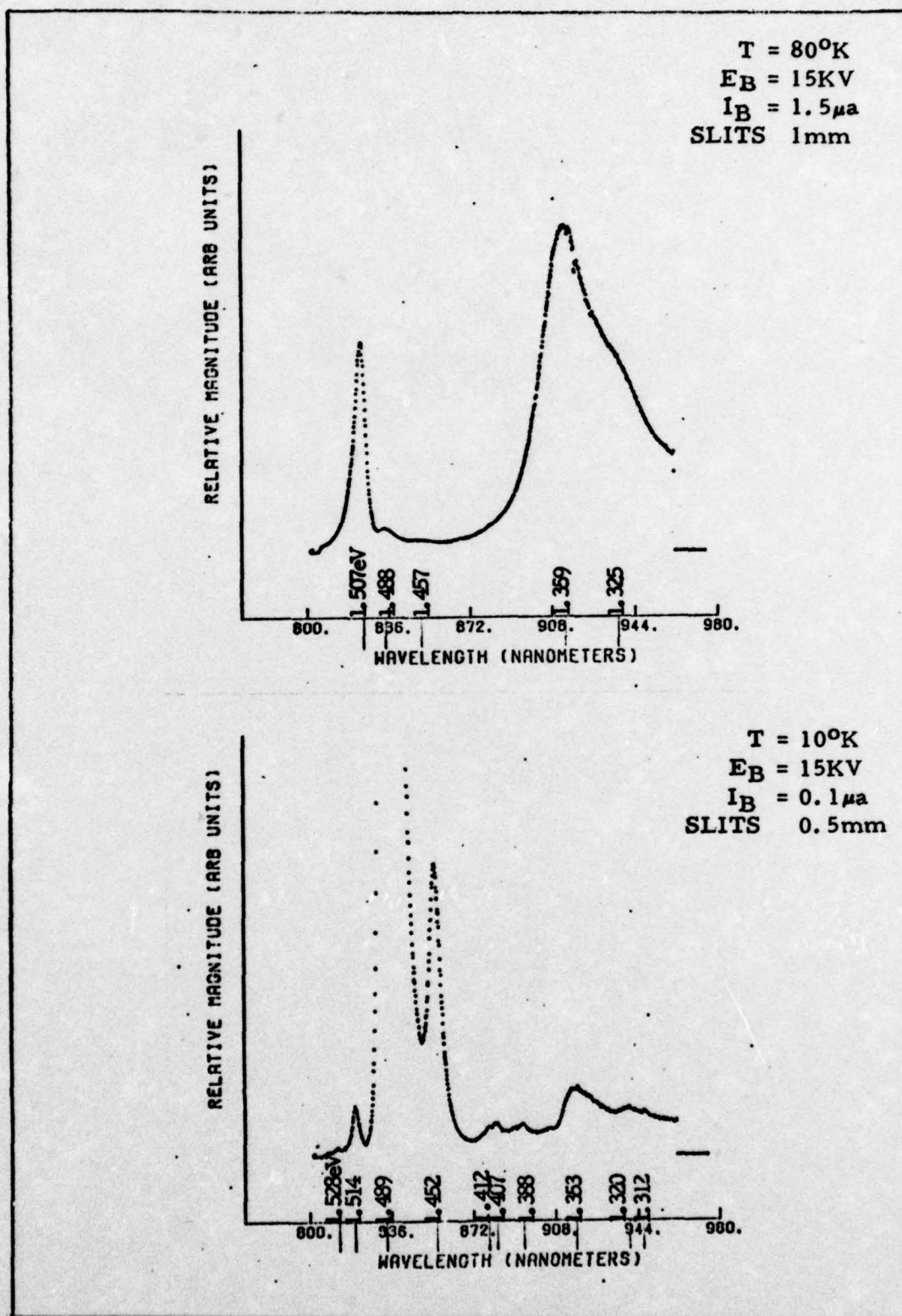


Fig. 6. Typical Spectra of Sample 8A at 10°K and 80°K

band to split. The strain between the Si_3N_4 cap and GaAs could be causing the 1.53eV peak in this case. The absence of this peak in sample 8AA is in agreement with the polishing results of Sturge; however, the 15 minute anneal data shows an increase in intensity over the unannealed sample for all fluences which is in disagreement with Sturge's polishing effect.

A peak at approximately 1.488eV is found in the 10°K spectra of samples 8 and 8A. The intensity of this peak greatly increases with annealing as shown in Table III on page 54. This fact together with the proximity of the 1.488eV peak to the 1.49eV Cd peak identified in the literature (Ref 4, 15) indicates that a cadmium acceptor is responsible for the 1.488eV peak. Also, the band gap decreases approximately 0.8meV from 80°K to 10°K (Ref 32:770) while the 1.489eV peak in sample 8A changes in energy by only 0.001eV. Therefore, the 1.488 eV peak is attributed to a donor-cadmium acceptor recombination (Ref 13, 14, 34, 36). The 1.452eV peak in the 10°K spectra is assigned to a longitudinal optical (LO) phonon replica of the 1.488eV peak, since the LO phonon energy in GaAs is approximately 36meV (Ref 4:33, 9, 15:827).

The 1.41eV peak and the 1.39eV peak at 10°K appear at all depths probed in the three samples. The intensity of these two peaks does increase with annealing, and is greatest near the sample surface (Table III). Therefore, these two peaks are attributed to As/Ga vacancies created by ion implantation and outdiffusion of As/Ga

through the Si_3N_4 cap during annealing (Ref 1:145-146, 8:144, 12).

The peak near 1.35eV at 10°K while increasing by 3meV with annealing for this set of data shows no such pattern at other depths in these samples, and no such pattern at any depth in the other samples. The intensity of this peak does increase with annealing, but at a slower rate than the Cd peak at 1.49eV. The intensity of the 1.35eV peak in the unimplanted sample is significantly larger than in any of the implanted samples. In the literature there appear two conflicting views as to the source of this peak. Based upon the enhancement of the 1.35eV peak with heat treatment in ampoules containing Cu impurities (Ref 11:320) and photoluminescence studies of defects in undoped GaAs (Ref 20:5356, 35:393) some researchers have concluded that transitions from the conduction band to copper acceptors cause the 1.35eV peak. Others have assigned the 1.35eV to Ga vacancies. This assignment was based on studies of luminescence data from Cu doped impurities and native defects in annealed and unannealed GaAs (Ref 8:144, 10:1422-1423). The increase of the 1.35eV peak intensity with annealing (Table III) supports the view that this peak is due to a vacancy. Further, the fact that the large intensity of this peak in the unimplanted sample decreases significantly upon Cd implantation indicates that Cd ions are filling the vacancies. Therefore, it is concluded that the 1.35eV peak is caused by Ga/As vacancies both native to the GaAs and enhanced through outdiffusion during annealing. There is also a peak at 1.37eV in the literature that has been attributed

to both Cu acceptors and vacancies (Ref 8:144, 21:832, 37:273). While in some cases the 10°K data shows a 1.36eV peak rather than the 1.35 eV peak there is no evidence for a 1.37eV peak in any of the samples studied. The 1.32eV peak is believed to be a LO phonon replica of the 1.35eV peak. This LO phonon has less energy than the normal LO phonon, 0.033eV in samples 8 and 8A versus 0.036eV, because of lattice perturbations near the vacancy complex (Ref 21:829). The 1.31eV peak is thought to be caused by a transverse optical (TO) phonon replica of the 1.35eV peak which has an energy of 0.010eV (Ref 24:3061).

Cadmium Implanted GaAs with Fluence = 10^{14} ion/cm². Typical spectra for samples 4 and 4A at 10°K and sample 4A at 80°K are shown in Fig. 7 on the following page. The same peaks appear in the annealed and unannealed spectra. The peak at 1.489eV shows the same temperature relationship between 10°K and 80°K as the 1.488eV peak in the 10^{12} ion/cm² fluence samples; and therefore, it is assigned to a donor-cadmium acceptor recombination. All other peaks appearing in the 10^{14} ion/cm² fluence sample spectra were found in the 10^{12} ion/cm² fluence sample spectra. And since the intensity changes of these peaks with annealing are very similar to the intensity changes found in the similar peaks of the 10^{12} ion/cm² fluence samples, the same recombination centers are considered responsible in both sets of samples.

Cadmium Implanted GaAs with Fluence = 10^{15} ion/cm². Typical spectra for samples 6 and 6A are shown in Fig. 8 on page 33. The

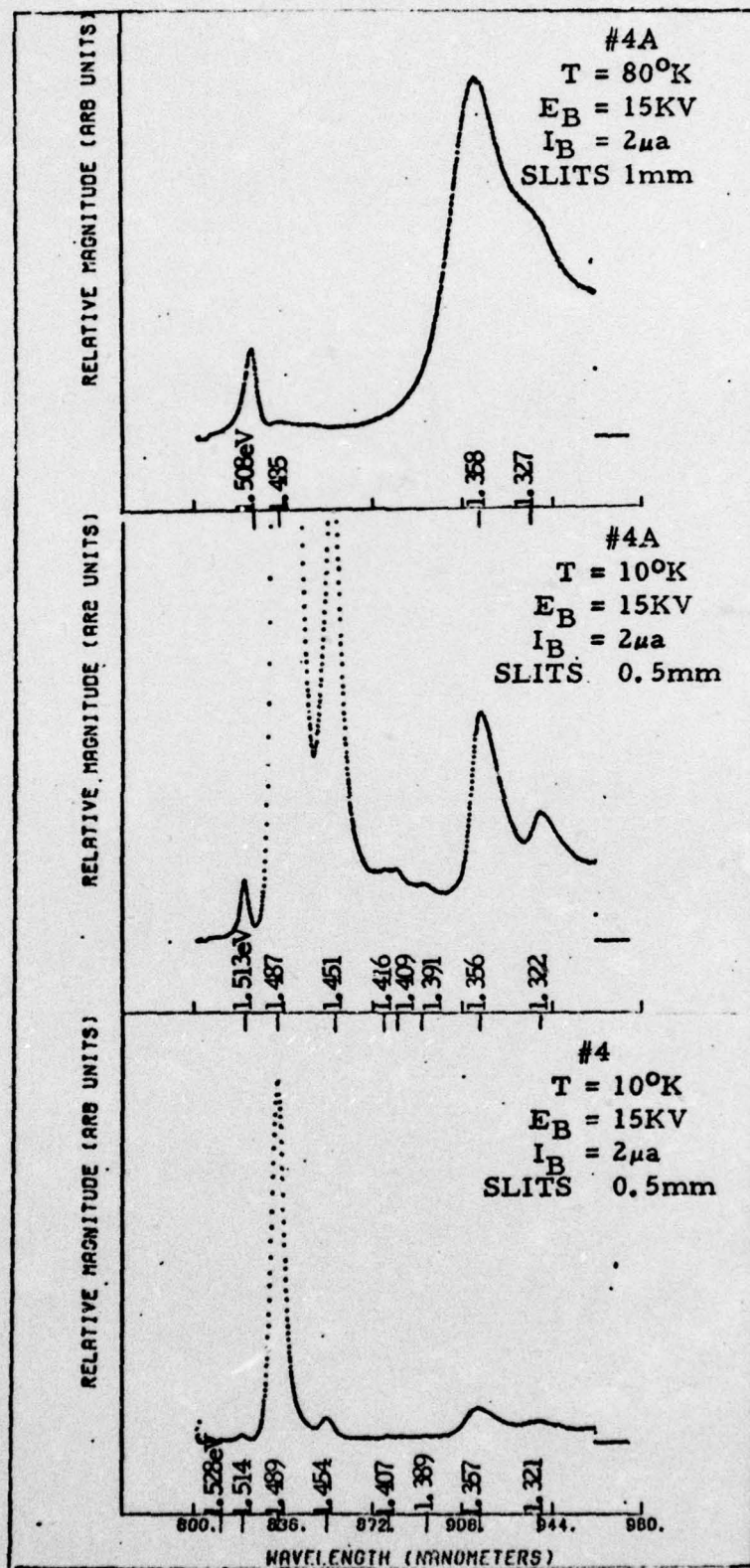


Fig. 7. Typical Spectra of Sample 4 at 10°K and Sample 4A at 10°K and 80°K

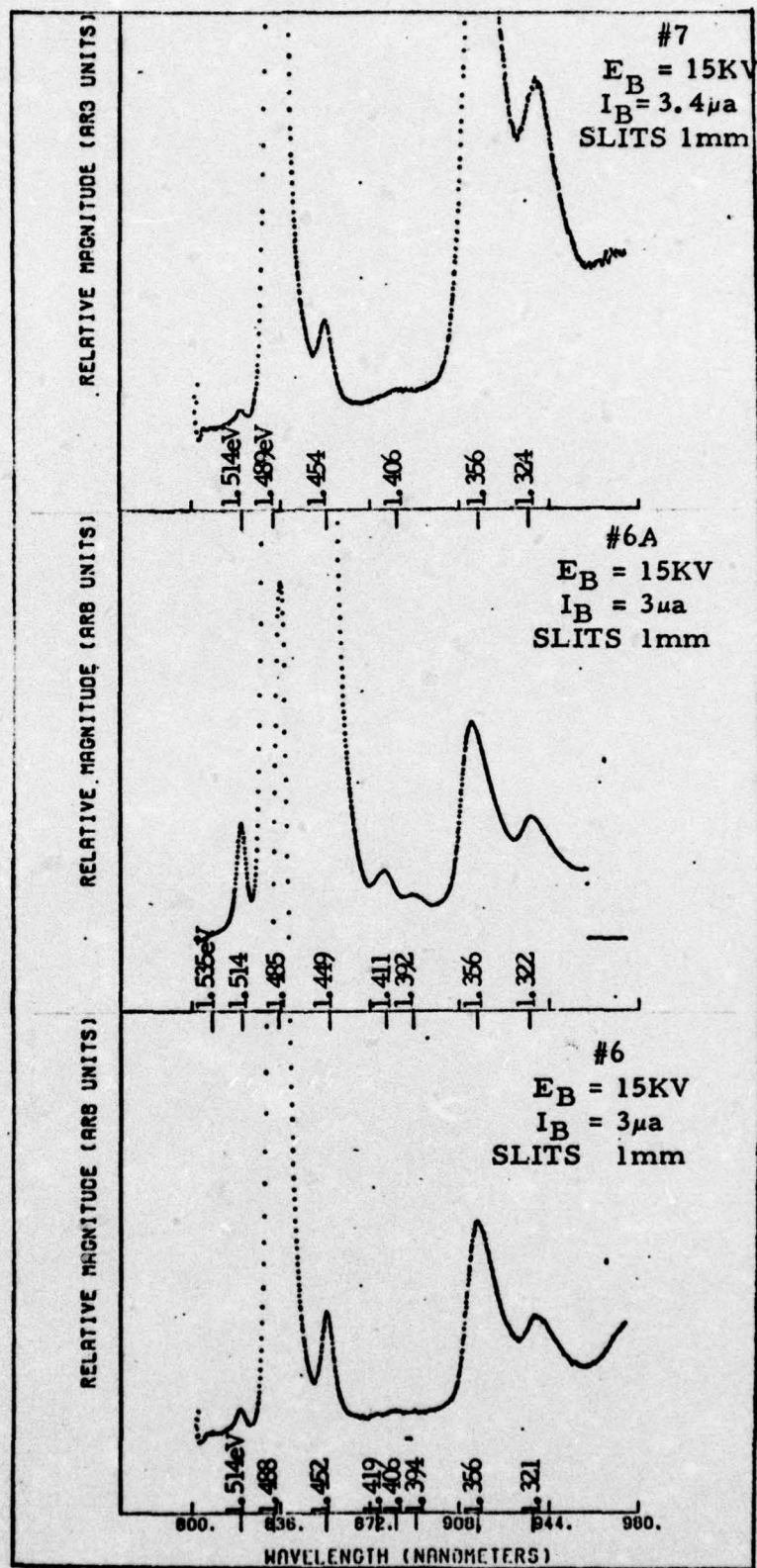


Fig. 8. Typical Spectra of Samples 6, 6A and 7 at 10°K

peaks which appear are very similar in energy to those peaks found in the cold implant spectra. The reason for the 1.53eV peak not appearing in the unannealed sample spectrum while appearing in the annealed sample spectrum is not known. All peaks are assigned to the same causes as were stated for the similar peaks in the cold implants. At all sample depths examined the 1.49eV peak is at approximately 3meV lower energy in the annealed sample spectrum than in the unannealed sample spectrum. The reason for this shift to lower energy becomes apparent when one examines the spectra presented in Fig. 9 on page 35. At a 7.5KV beam energy a shoulder at 1.470eV becomes visible on the 1.49eV peak. This shoulder becomes totally resolved as a peak at 1.464eV for a 5KV beam energy. At 4.75KV the energy of this peak is 1.458eV. It is this peak on the lower energy side of the 1.49eV peak that shifts the 1.49eV peak energy to the lower values found in the annealed sample. The 1.46eV value is the energy of the shoulder peak in all spectra shown, but the more intense 1.49eV peak at higher electron beam energies masks the true 1.46eV value. This value becomes apparent only when the 1.49eV peak intensity is considerably weakened at 4.75KV. The 1.46eV peak appears in the spectrum of the unimplanted unannealed sample as well. This peak is assigned to a vacancy native to the 'as grown material' which is enhanced by high fluence ion implantation and annealing (Ref 9:568, 10:1422).

Cadmium Implanted GaAs with Fluence = 10^{16} ion/cm². A typical 10°K spectrum for sample 7 is shown in Fig. 8. An annealed sample at

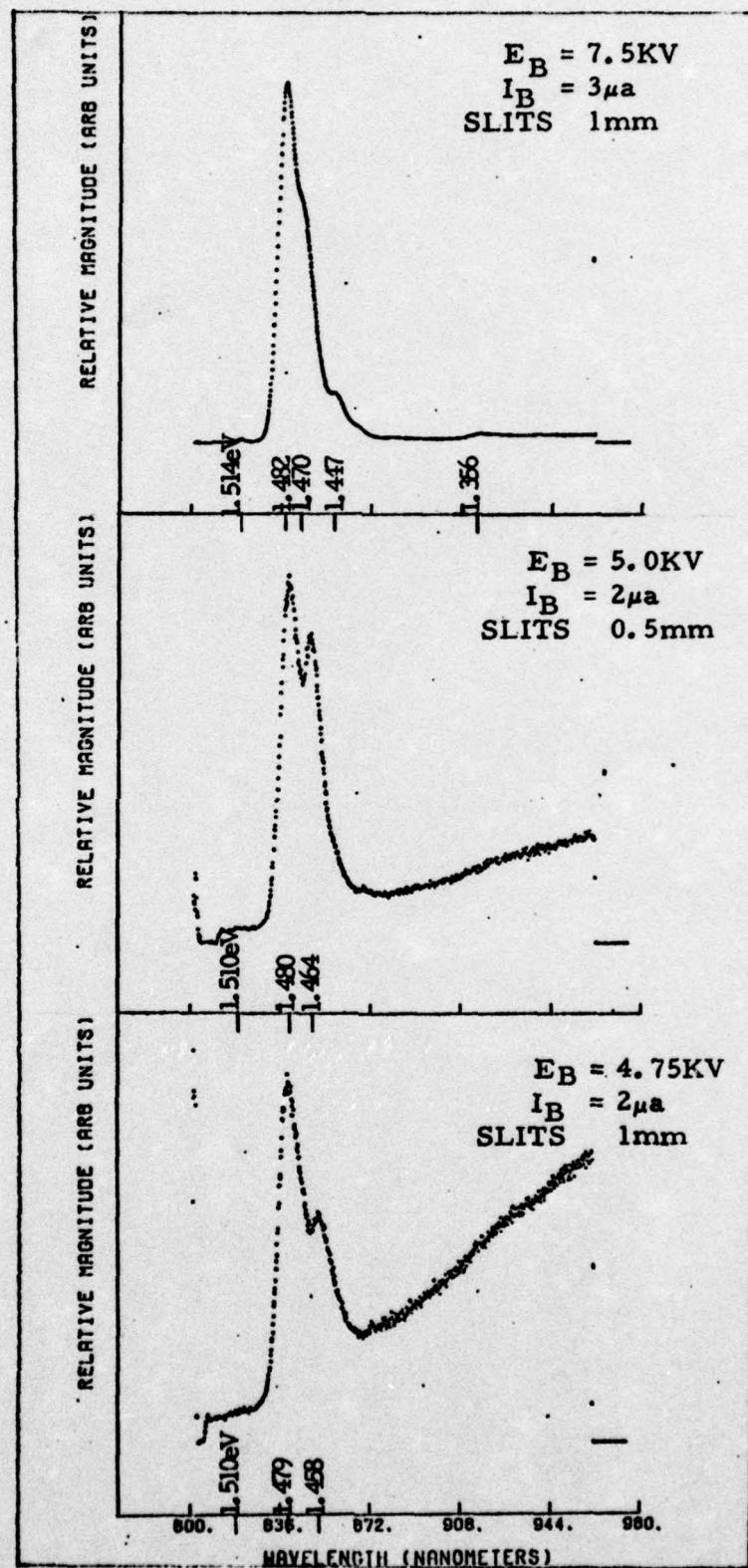


Fig. 9. Depth Resolved Spectra of Sample 6A at 10°C

this fluence was not examined. The peaks in this spectrum are almost identical to the peaks in the 10^{15} ion/cm² fluence sample spectra. The absence of the 1.53eV peak is consistent with the results of the 10^{15} ion/cm² fluence unannealed sample.

Unimplanted GaAs. Typical spectra for samples 11 and 11AC at 10°K are shown in Fig. 10 on the following page. The peaks have very similar energies in both spectra. From arguments made previously the peaks are identified as follows: 1.514eV--unresolved exciton/conduction--valence band recombination; 1.46eV, 1.41eV, and 1.36eV--native defects due to Ga/As vacancies; and 1.32eV--LO phonon replica of the 1.36eV peak. Except for the 1.39eV peak all other peaks associated with lattice damage in the ion-implanted samples are present in sample 11. These peaks are believed to be caused by native defects in sample 11 since their intensities increase with annealing as seen in the intensity data presented in Table III for samples 11 and 11AC. The absence of the 1.39eV peak from the spectra of samples 11 and 11AC indicate that this is the only peak which is caused entirely by damage from ion implantation and annealing. The 1.38eV peak in the sample 11AC spectrum may be associated with the 1.39eV peak. Its presence in all of the sample 11AC spectra and in none of the sample 11 spectra is a strong argument for associating it with vacancies which are formed by outdiffusion of Ga/As with annealing. The reason for the high intensity of the 1.36eV peak compared to the other peaks assigned to vacancies, or even to the 1.49eV peak, is not known. However, it is

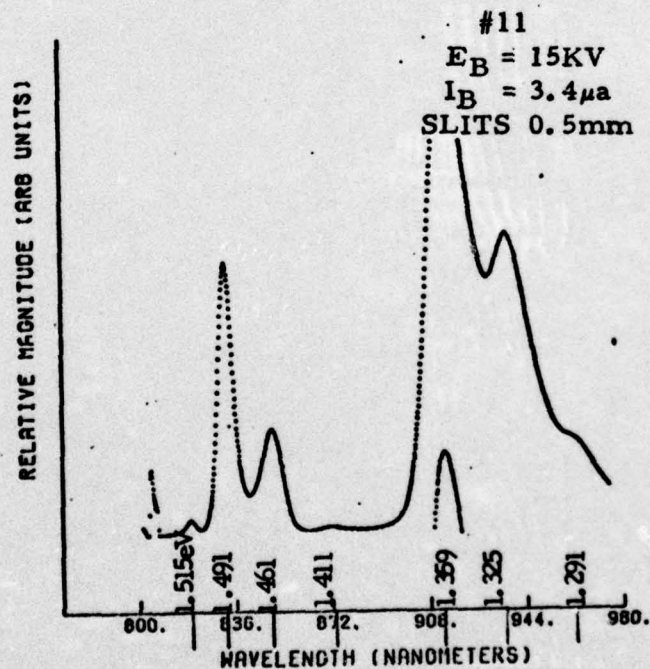
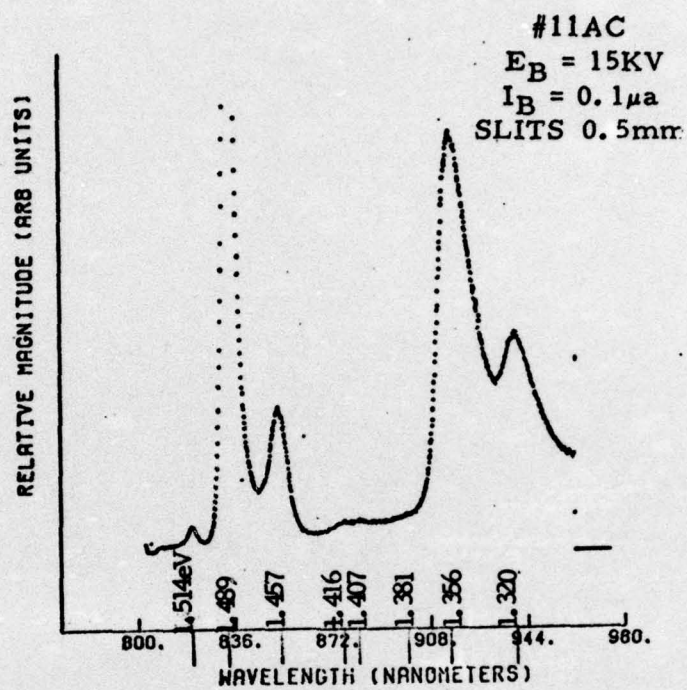


Fig. 10. Typical Spectra of Samples 11 and 11AC at $10^{\circ}K$

not unusual for a sample, like 11, which is not epitaxial to contain strong and numerous peaks due to both native defects and impurities. The 1.49eV peak could be caused by any number of impurities which have a characteristic energy peak at 1.49eV. Some of the possibilities are: Si (Ref 3:997, 8:144, 20:5348), Be (Ref 9:568), Zn (Ref 15:788), and of course, Cd (Ref 4, 15). In this case the 1.49eV peak is attributed to Si since only Si has been identified as the impurity responsible for the 1.49eV peak when this peak has been found in undoped samples of GaAs (Ref 3:977, 8:144).

Damage Layer

Table II on the following page contains the 1.49eV peak intensities and base line intensities of those spectra which are believed to show the damage layer produced by the ion implantation of GaAs. The base line spectrum is produced by the optical emission from the electron gun cathode, and it is shown in Fig. 12 on page 42. Except for samples 4 and 7 there is intensity data from two spectra for each sample. The two chosen were: the spectrum most resembling the electron gun spectrum but still showing peaks attributed to the GaAs spectrum, and the spectrum produced by the next lowest energy electron beam used. The spectra for samples 11 and 11AC are presented as a comparison of unimplanted versus implanted samples. The ratio of base line intensity to 1.49eV peak intensity is also shown for each spectrum in Table II. By comparing the changes in the actual spectra

Table II
Damage Layer Depths--All Samples, 10°K

Sample GaAs #	E _B (KV)	I _B μa	Intensity (# of counts)		Ratio Base/1.49	E _B -1.5 (KV)	Depth In GaAs (μm)
			1.49eV	Base			
8	2.5	1	1340	1000	0.75	1.0	0.03
8	2.0	1	1008	900	0.89	0.5	0.01
4	7.5	2	2942	1700	0.58	6.0	0.37
4	6.0*					4.5*	0.24
6	8.0	3	2166	1900	0.88	6.5	0.42
6	7.5	3	1526	1400	0.92	6.0	0.37
7	12.5	3	5587	2300	0.41	11.0	0.89
7	10*					8.5*	0.61
11AC	2.0	1	6627	2300	0.35		
11AC	1.5	0.9	1753	1500	0.86		
8AA	1.75	1	1762	1200	0.68	0.25	0.004
8AA	1.5	0.9	1313	1000	0.76	0	0
4A	4	1	2416	1100	0.45	2.5	0.10
4A	3	1	---	800	---	1.5	0.05
6A	4.5	2	4314	1500	0.35	3.0	0.13
6A	3.5	2	1275	1200	0.94	2.0	0.07

*Estimated value

to the ratio changes presented in Table II for these spectra it is concluded that a ratio greater than 0.75 is a good indication that the luminescence is from a layer within 0.5eV of the damage layer, and a ratio greater than 0.85 indicates that the luminescence is from the boundary region of the damage layer. In the damage layer no luminescence from the GaAs sample is present and only the optical emission from the electron gun cathode is detected. Using the scheme developed in Chapter II, the beam energy at which the ratio of the base

line intensity to the 1.49eV peak intensity is greater than 0.85 is converted to the corresponding depth of penetration into the GaAs crystal; and this depth is considered the maximum extent of the damage layer in the sample. There are two cases where insufficient data makes it necessary to estimate the depth of the damage layer. These estimates are more qualitative than quantitative; however, they are based upon two experimental observations. First, for most of the spectra which have ratios below 0.5 only a drop in beam energy of 0.5KV to 1KV is needed to move the ratio above 0.85. Second, the further the damage layer extends from the crystal surface the slower is the approach to the 0.85 ratio from the 0.5 ratio. The accuracy of the depth layer measurements are estimated at ± 0.25 KV. Much of this uncertainty is due to the poor resolution of the beam voltage meter.

Cadmium Implanted GaAs with Fluence = 10^{12} ion/cm². In Fig. 11 and Fig. 12 on the following pages are the spectra for samples 8 and 8AA respectively, which are used to calculate the damage layer depth in Table II. Also shown in Fig. 12 is the electron gun spectrum. Damage layer data was not obtained on sample 8A. The change in luminescence of sample 8 from 2.5KV to 2KV illustrates the failure of the electron beam to penetrate the damage layer at an energy of 2KV. The 0.01 μ m damage layer depth corresponds to a concentration of 2.6×10^{17} ion/cm³ from LSS theory. The damage layer appears to be completely removed by a 30 minute 800°C anneal as illustrated by the continued presence of a rather strong 1.49eV peak at a 1.5KV beam

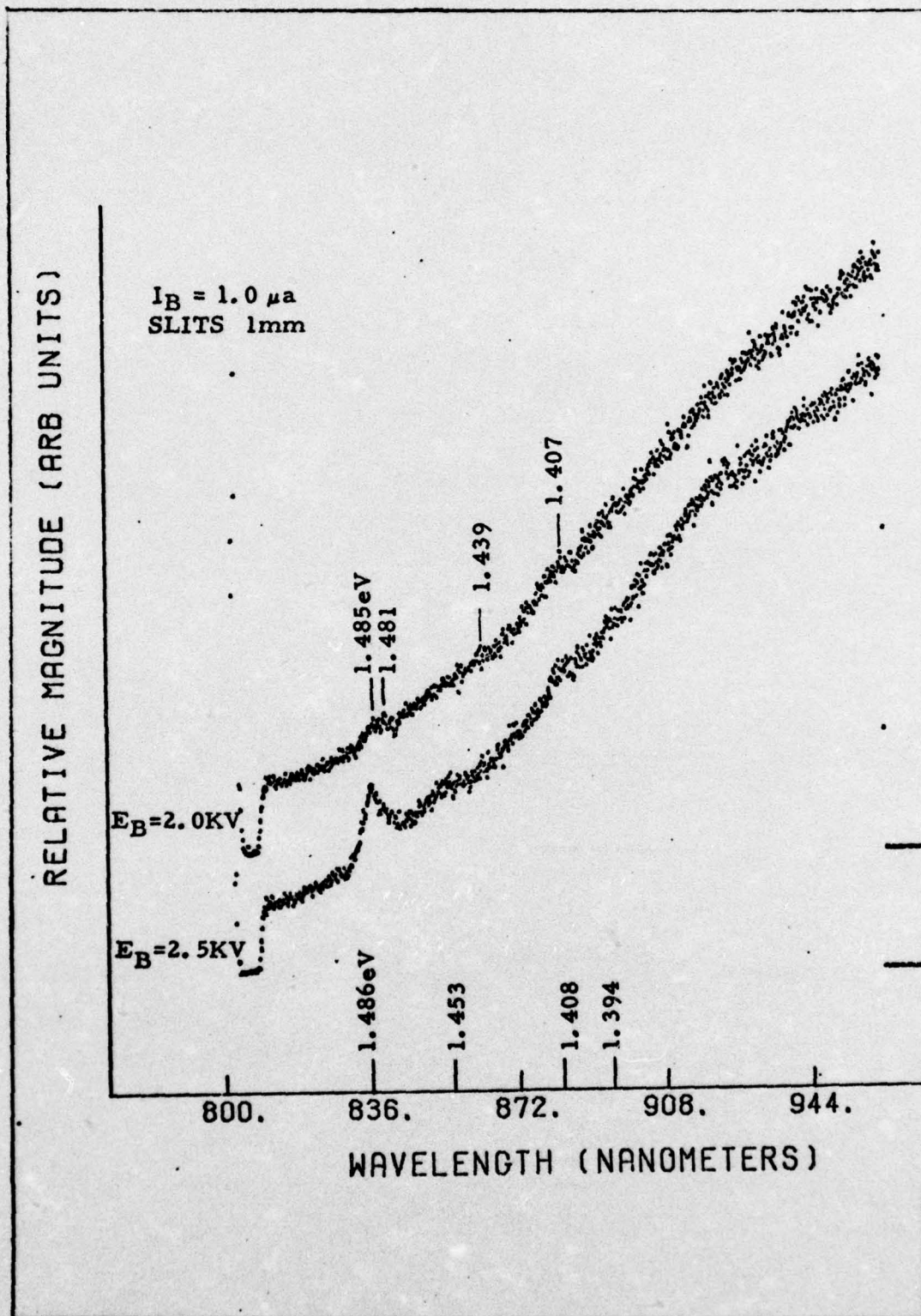


Fig. 11. Damage Layer Spectra of Sample 8 at 10°K

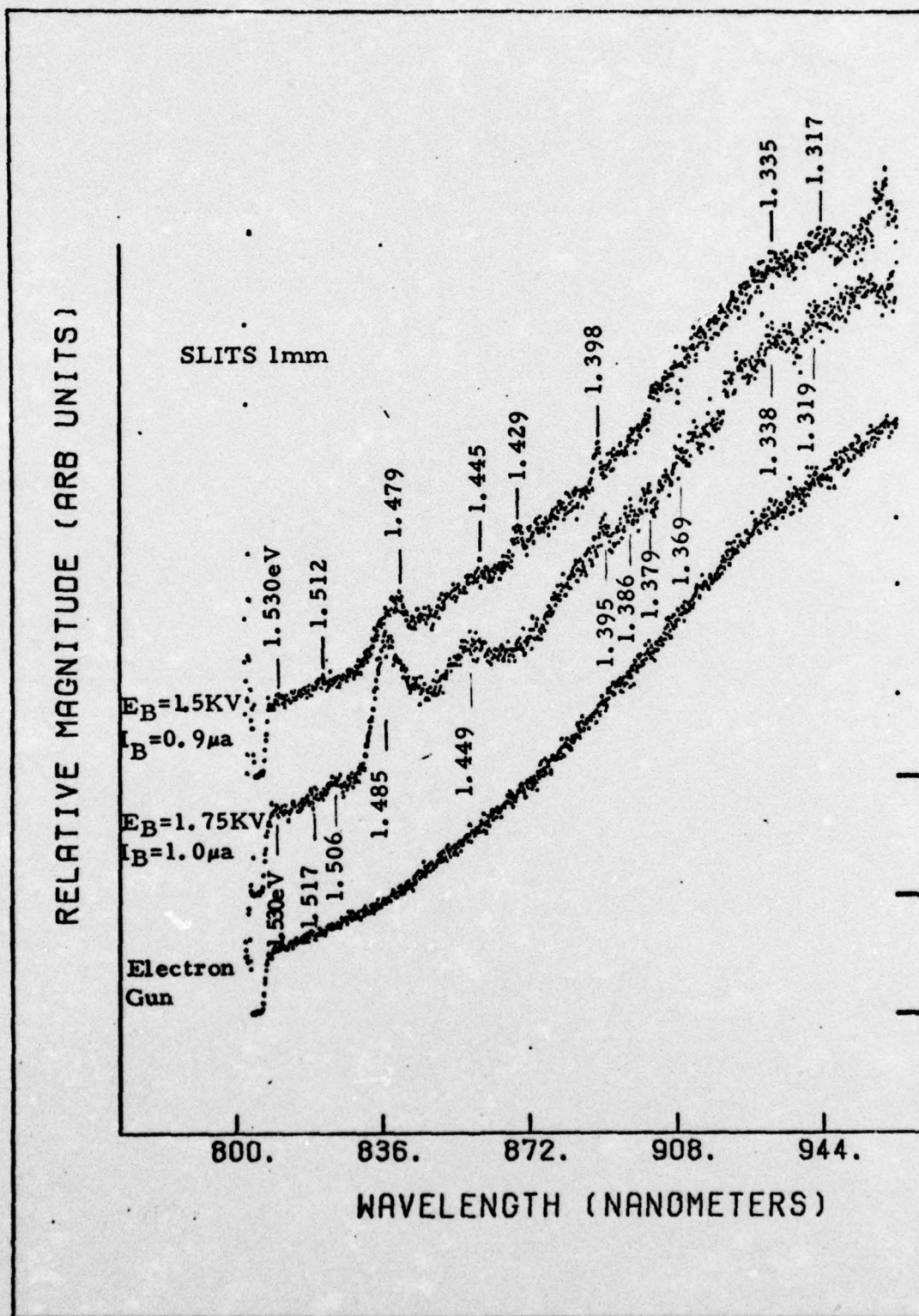


Fig. 12. Damage Layer Spectra of Sample 8AA at 10°K

energy. The reason for the shift of the 1.49eV peak to lower energy is not known. In Chapter II it was calculated that 1.75KV electrons were needed to penetrate the 300 Å Si_3N_4 cap. It is obvious from this luminescence at 1.5KV that the cap had already been penetrated. This discrepancy can be due to instrumentation error, which is significant at such low energies, or to error in the theory. It is also possible that the cap is not 300 Å thick. Time did not permit the thickness of the cap to be determined by another experimental method.

Cadmium Implanted GaAs with Fluence = 10^{14} ion/cm². The spectra for samples 4 and 4A which were used in Table II are presented in Fig. 13. The sample 4 spectrum, except for the relatively strong Cd peak at 1.488eV, has the characteristic shape of the electron gun spectrum, indicating that most of the electrons are stopping inside the damage layer. Unfortunately, further data could not be collected to more accurately define the damage layer; and therefore, it had to be estimated. The 6KV estimate, based upon the experimental observations mentioned earlier; is believed to be well within the damage layer. The damage layer is calculated to extend 0.24 μm into the GaAs material. This is an increase by a factor of 20 over the depth of the damage layer in the 10^{12} ion/cm² fluence sample. According to LSS theory the concentration at a depth of 0.24 μm in the 10^{14} ion/cm² fluence sample is less than 10^{-33} ion/cm³. It is difficult to understand how such an ion density could produce enough damage to quench luminescence so effectively. The 2.6×10^{17} ion/cm³ concentration calculated from

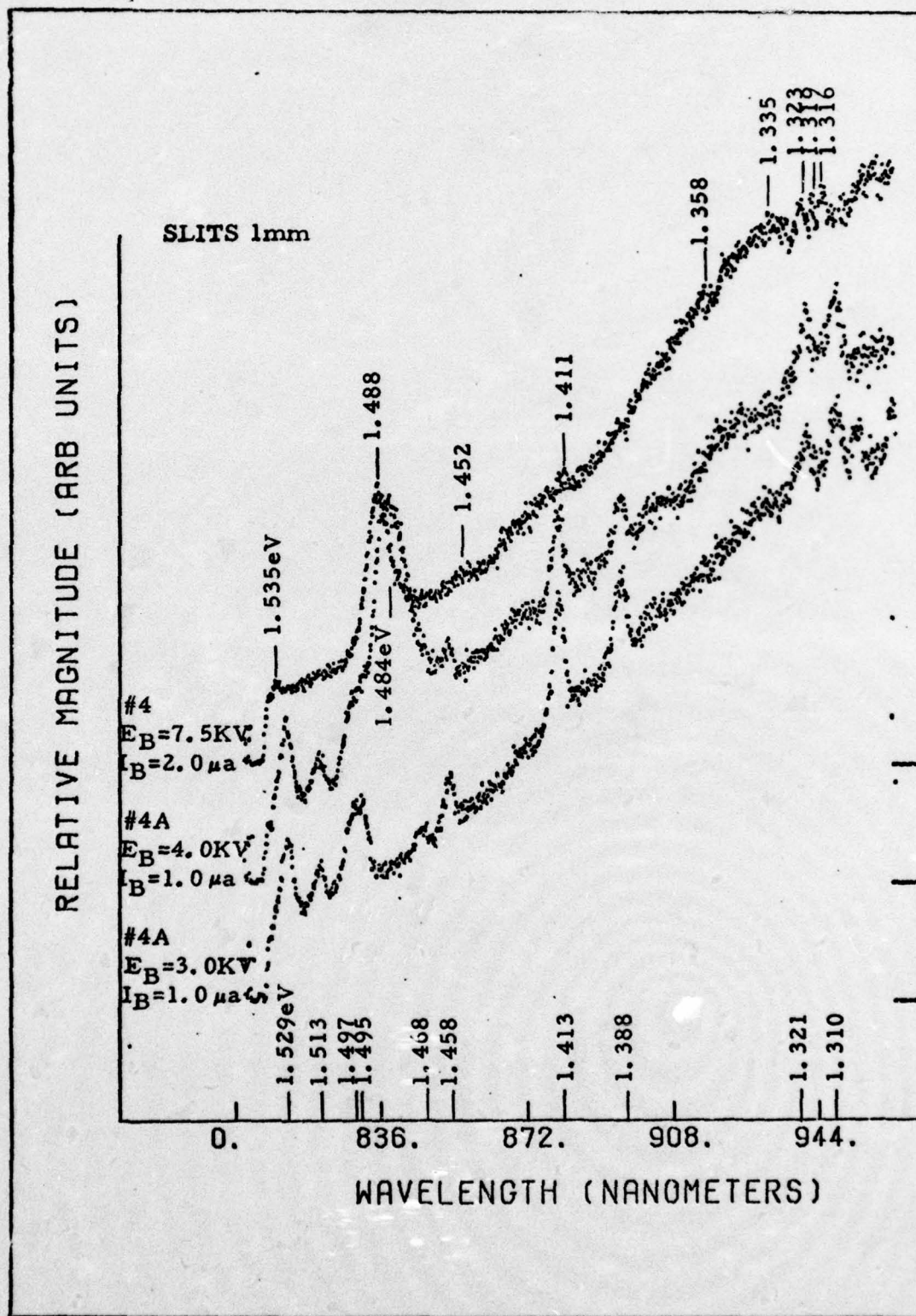


Fig. 13. Damage Layer Spectra of Samples 4 and 4A at 10°K

LSS theory for the 10^{12} ion/cm² fluence sample seems much more likely to be able to cause a damage layer than the 10^{-33} ion/cm³ value. It seems evident that LSS theory does not give the correct penetration profile for Cd implantation in this sample. Of course there is also the possibility that this loss of luminescence is not due to a damage layer. This cannot be the case since the increase of the luminescence quenching depth with increasing fluence in the unannealed samples, and the significant decrease of this luminescence quenching depth with annealing for each fluence sample strongly support an ion implantation damage layer as the cause. Further, the damage layer depth and the failure of LSS theory found in this study are substantiated by Hanson who, using an electroreflectance technique, found that the damage caused by a room temperature 120KV Cd implantation into GaAs at a fluence of 10^{14} ion/cm² extended to a depth of 0.20 μ m. He also noted that LSS theory did not predict the long tail on the experimental damage profile (Ref 19:58).

The 4A sample spectra at 4KV and 3KV are an excellent illustration of the transition into the damage layer. The sharp energy peaks which appear in both spectra clearly illustrate the damage peaks referred to in the previous section. The peak at 1.484eV in the 4KV spectrum completely disappears in the 3KV spectrum and is replaced by peaks at 1.496eV and 1.468eV. The 1.468eV peak is believed to be caused by the same vacancy complex responsible for the 1.46eV peak in sample 6. The 1.496eV peak could be caused by a conduction

band-Si acceptor as mentioned for sample 11 but it does seem a little high for such an assignment. The important point is that the 1.484eV peak is no longer present and many peaks due to damage are strongly visible, riding on the electron gun spectrum. This indicates that at 3KV the electron beam penetrates just to the edge of the damage layer. The annealing at 800°C for 15 minutes is not enough to eliminate the damage layer completely but the anneal does reduce it to a layer extending 0.05 μm below the surface. This is still 0.04 μm greater than the unannealed 10^{12} ion/cm² fluence damage layer. This inability of an 800°C anneal to eliminate damage caused by a low fluence implant is substantiated by K. Aoki et al, who found that defects produced by a 2×10^{13} ion/cm² fluence could not be eliminated by an 800°C anneal for 15 minutes in flowing hydrogen gas (Ref 1:146).

Cadmium Implanted GaAs with Fluence = 10^{15} ion/cm². Sample 6 and sample 6A spectra used in Table II are shown in Fig. 14 and Fig. 15 respectively on the following pages. In sample 6 the 1.486 eV peak almost totally disappears between a beam energy of 8KV and 7.5KV. The usual damage peaks are again quite intense compared to the 1.486 eV peak. In the 7.5KV spectrum the peaks at 1.493eV and 1.485eV could be the band-acceptor and donor-acceptor recombinations respectively for a Si acceptor (Ref 3:997, 20:5348), rather than peaks due to Cd. The damage layer is calculated to extend 0.37 μm into the crystal. This is a 0.13 μm increase in depth over the 10^{14} ion/cm² fluence sample damage layer. The small increase in the damage

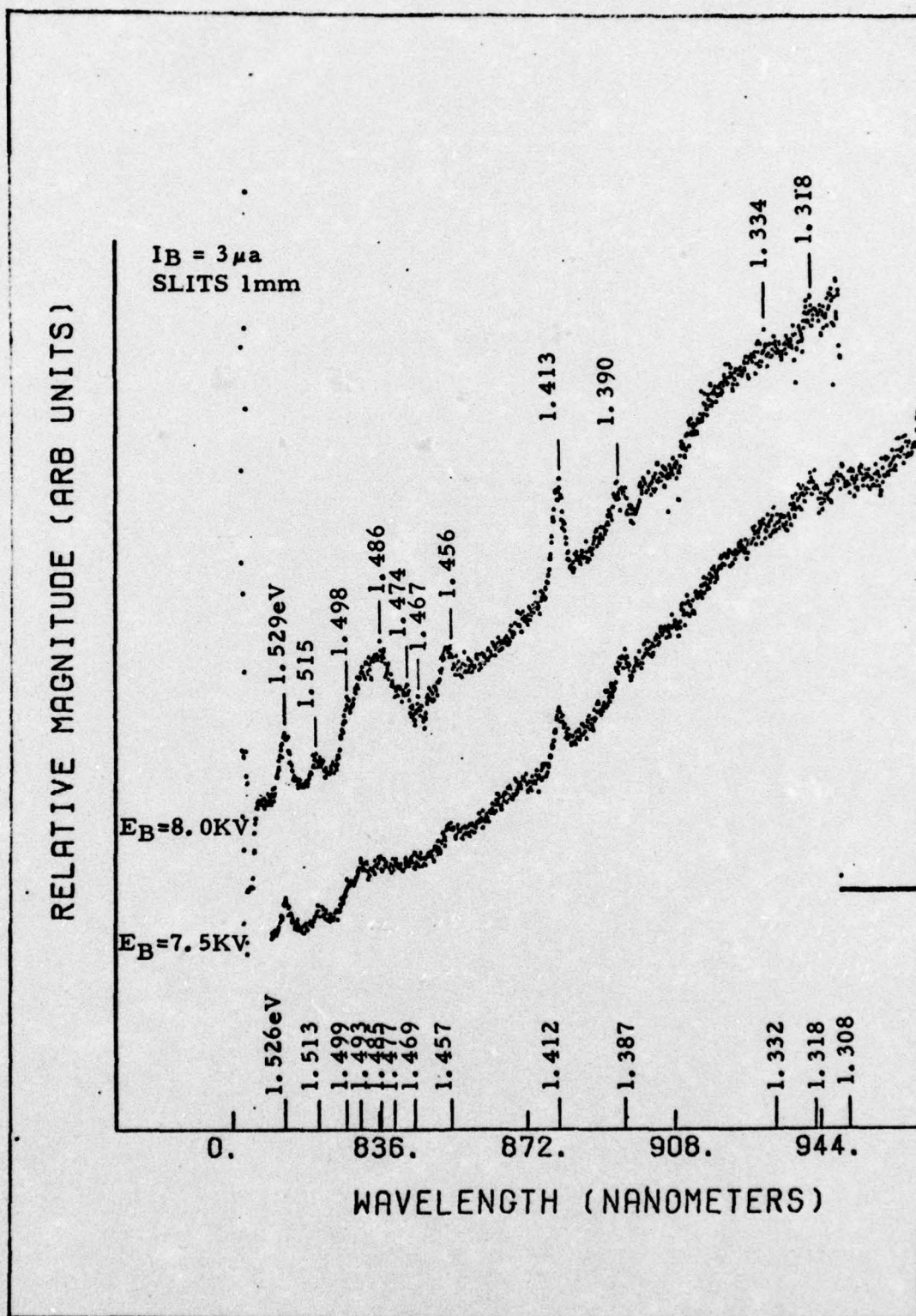


Fig. 14. Damage Layer Spectra of Sample 6 at 10°K

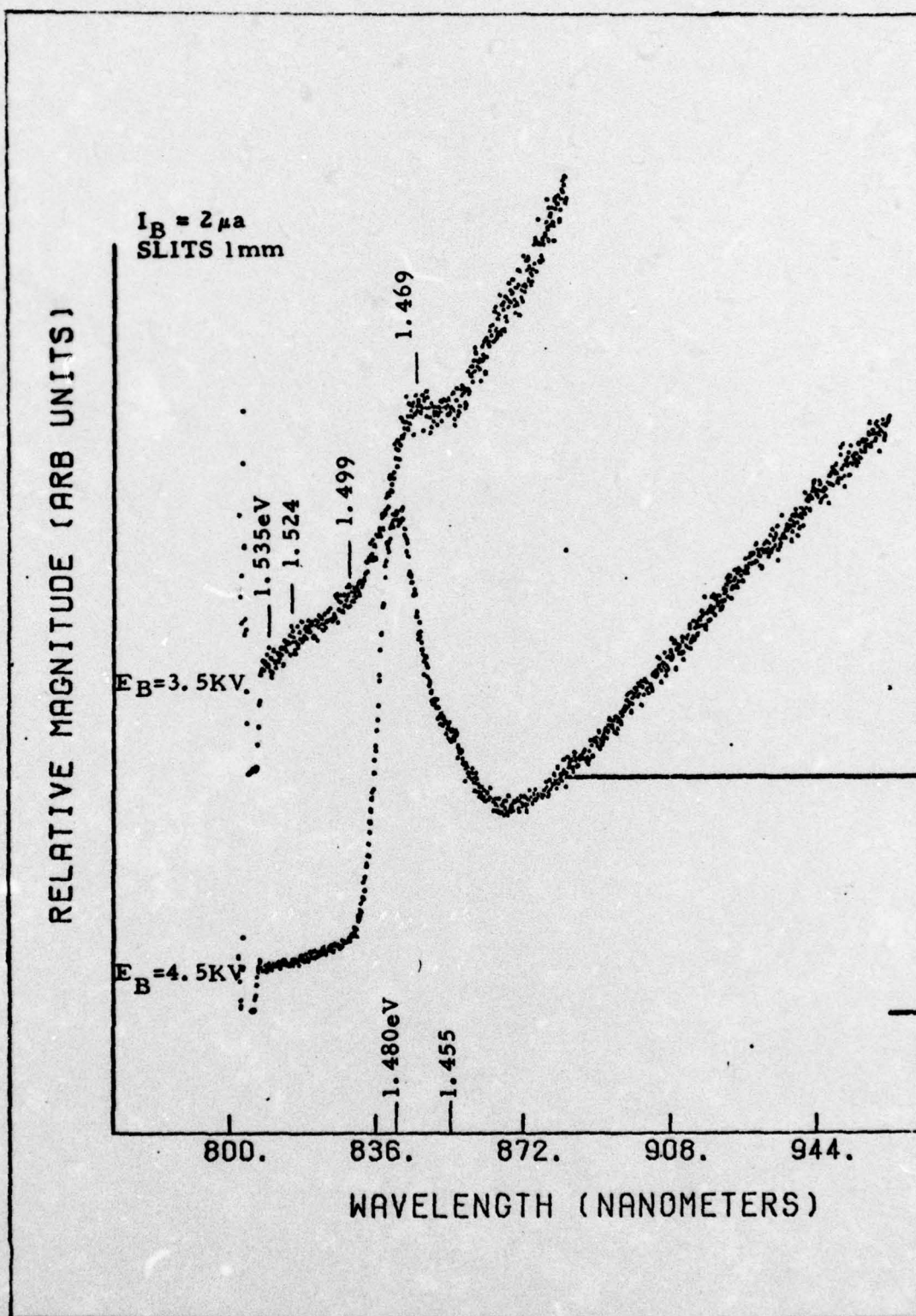


Fig. 15. Damage Layer Spectra of Sample 6A at 10°K

layer between these two samples as compared to the $0.23\text{ }\mu\text{m}$ increase between samples 8 and 4 and the $0.24\text{ }\mu\text{m}$ increase between samples 6 and 7 indicates that a hot ion implantation produces less damage than a cold one. To prove this beyond question would require the study of a hot and a cold ion implantation of the same fluence. The concentration of Cd ions at the depth where the damage layer ends is less than 10^{-99} ion/cm^3 according to LSS theory. This again demonstrates the failure of LSS theory to predict the correct Cd ion concentration profile.

For sample 6A the peak at 1.480 eV in the 4.5 KV spectrum is no longer present in the 3.5 KV spectrum, although a peak at 1.469 eV is evident. This peak is again identified as damage. These two spectra do show that the damage layer clearly extends to the 2 KV level in the GaAs crystal. This corresponds to a layer extending $0.07\text{ }\mu\text{m}$ below the crystal surface. This is only $0.02\text{ }\mu\text{m}$ deeper than in sample 4A, which is surprising considering that before annealing sample 6 had a damage layer that extended $0.13\text{ }\mu\text{m}$ deeper than the damage layer of sample 4. It is possible that the damage layer of a hot implant is more easily annealed out than that of a cold implant.

Cadmium Implanted GaAs with Fluence = 10^{16} ion/cm^2 . The spectrum for sample 7 at 12.5 KV is shown in Fig. 16 on the following page. The 1.49 eV peak is still very strong; however, no data is available at lower beam energies. The damage layer is estimated to end at 10 KV which corresponds to a depth of $0.61\text{ }\mu\text{m}$ in the crystal. This estimate is considered to represent the most extensive damage layer

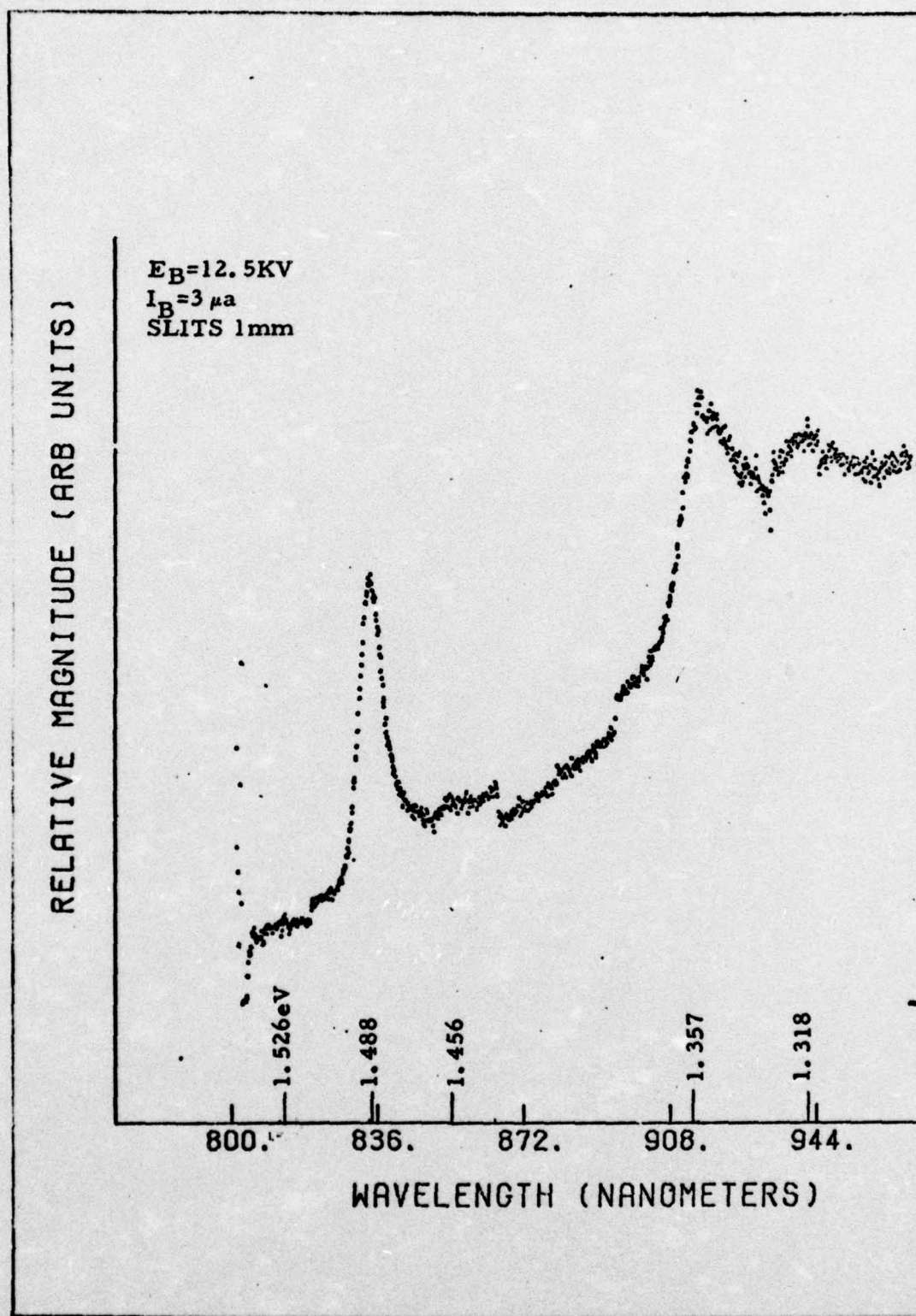


Fig. 16. Damage Layer Spectrum of Sample 7 at 10°K

possible for this case. As previously mentioned, the increase in the depth of the damage layer between samples 6 and 7 is greater than between samples 4 and 6 indicating that a hot implant produces less damage than a cold one.

Unimplanted GaAs. The spectra of sample 11AC presented in Fig. 17 on page 52 show that the 1.488eV peak intensity is considerably reduced as the electron beam energy is reduced from 2KV to 1.5KV. Since this sample was not Cd-implanted the reduction in intensity cannot be explained by an ion implantation damage layer. The intensity reduction is an indication of a dead layer for luminescence. This dead layer is due to the proximity of the carriers (electrons and holes) to the crystal surface. The time it takes the majority of the carriers produced by the electron beam to reach the crystal surface, where surface recombination dominates, is less than the mean lifetime of these carriers before recombination occurs by one of the means mentioned in Chapter II. The surface recombination does not produce luminescence, it is non-radiative. The fact that the electron beam cannot be controlled well at low energies is another factor, although minor compared to surface recombination, which helps to reduce the luminescence. At beam voltages below 2KV the width of the electron beam at the sample block is larger than the diameter of the hole in the mask covering the sample. This is in comparison to a beam at 5KV which is small enough to be positioned on different parts of the sample visible through the mask hole. The electrons lost to the mask can no

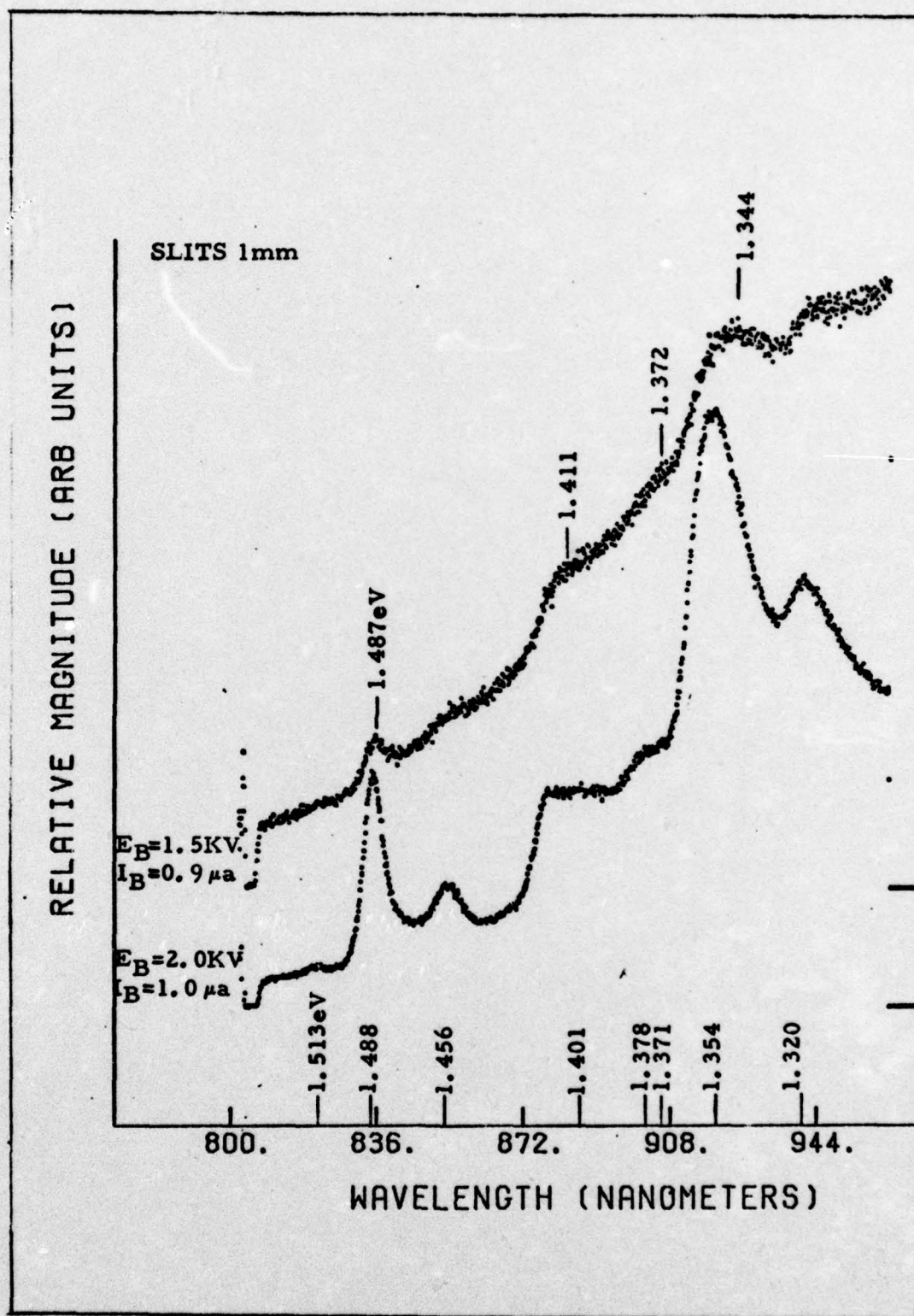


Fig. 17. Near Surface Spectra of Sample 11AC at $10^\circ K$

longer excite the sample; and therefore, the luminescence intensity drops. It should be noted that in sample 8AA luminescence of similar intensity to that found in the 1.5KV 11AC spectrum was estimated to be from the GaAs surface. This higher surface luminescence intensity in sample 8AA compared to sample 11AC is because the presence of the Si_3N_4 cap in sample 8AA reduced the amount of surface recombination from that found in sample 11AC. Further, the presence of the cap put the GaAs surface at a beam energy of 1.5KV, thereby reducing the electron beam expansion effect.

Annealing Effects

The investigation of the effects of annealing on the different samples studies was complicated by two factors. First, the occurrence of an intense peak at 1.49eV in the unimplanted sample meant that the intensity of the 1.49eV peak in the implanted and annealed samples was due to both Cd ions and the impurity which caused the original peak at 1.49eV. The intensity data at 15KV and 5KV presented in Table III on the following page shows that this original impurity peak at 1.49eV is not as great a factor in the higher beam energy spectra as it is in the lower ones. The second complicating factor was the lack of intensity data for the comparison of all samples under identical equipment settings. This is illustrated in Table III by the beam current and slitwidth changes as beam energy is varied and by the lack of data for some of the samples at many of the beam energies shown.

Table III
Intensities of Selected Peaks

Sample GaAs #	EB (KV)	I _B μa	Slit- width (mm)	Intensity (# Counts)					Ratios		
				1.49eV	1.35eV	1.413eV	1.407eV	1.39eV	1.35/1.49	1.407/1.49	1.39/1.49
8	25	0.1	0.5	43334	5401	1163	1085	1243	0.13	0.03	0.03
8A	25	0.1	0.5	180332	6092	1801	1709	1989	0.03	0.01	0.01
8AA	25	0.1	0.5	396149	55537	2309	2618	2332	0.14	0.01	0.01
8	15	0.1	0.5	22816	2288	1197	1016	1197	0.10	0.04	0.05
8A	15	0.1	0.5	251951	4917	2094	2319	2296	0.02	0.01	0.01
8AA	15	0.1	0.5	208676	18128	1627	1852	1662	0.09	0.01	0.01
4	15	2.0	0.5	69069	6679	1318	1139	1408	0.10	0.02	0.02
4A	15	0.1	0.5	94264	4842	2142	2208	1968	0.05	0.02	0.02
6A	15	0.1	0.5	47117	1943	--	1099	1106	0.04	0.02	0.02
11AC	15	0.1	0.5	42497	24954	1814	1900	2014	0.59	0.04	0.05
8	10	3	1	132803	14132	--	3393	3408	0.11	0.03	0.03
6A	10	2	1	647955	18253	--	9551	6701	0.03	0.01	0.01
11	10	2	1	17895	112571	--	7258	7860	6.29	0.41	0.44
11AC	10	2	1	336010	395239	15309	14777	--	1.18	0.04	--
4A	10	2	0.5	352134	24372	11895	11945	9135	0.07	0.03	0.03
8A	5	2	0.5	182000	8125	2648	2533	2376	0.05	0.01	0.01
8AA	5	2	0.5	216678	25552	2127	2226	1966	0.12	0.01	0.01
4A	5	2	0.5	16723	2531	--	2078	1816	0.15	0.12	0.11
6A	5	2	0.5	7268	--	--	--	--	--	--	--
11AC	5	2	0.5	43244	56377	6204	5968	5753	1.30	0.14	0.13
4A	4	1	1	2461	--	2386	--	2439	--	0.97	0.99
4A	3	1	1	1307	--	2586	--	2747	--	1.98	2.10

Cadmium Implanted GaAs with Fluence = 10^{12} ion/cm². The data in Table III at 25KV and 15KV clearly show that the intensity of the 1.49eV peak in sample 8 increases drastically with annealing at 800°C for 15 minutes. Peaks associated with lattice vacancies also increase in intensity with this anneal. The decrease in the ratio of the 1.35eV peak to the 1.40eV peak is probably caused by more vacancies being filled by Cd ions than are created by outdiffusion of GaAs during the anneal. Annealing sample 8A for an additional 15 minutes decreases the 1.49eV (Cd) peak intensity at 15KV while increasing it at 25KV and 5KV. The increase in intensity at 5KV is probably caused by a further decrease in damage near the surface of the crystal. The increase in intensity at 25KV with the decrease in intensity at 15KV could indicate that Cd ions are diffusing from the 15KV layer to the layer between 15KV and 25KV faster than the damage is being decreased in the 15KV layer. But data on longer anneals for all samples are necessary before this trend seen in the 10^{12} ion/cm² fluence samples can be confirmed and the cause firmly established.

At all beam energies sample 8AA shows an increase over sample 8A in the ratio of the 1.35eV peak to the Cd peak. This may indicate that with an 800°C anneal for longer than 15 minutes outdiffusion of Ga/As cannot be compensated for by the filling of vacancies with Cd ions. The ratio of the intensities of the 1.407eV peak and the 1.39eV peak to the Cd peak remains constant with additional annealing at all electron beam energies. The peaks at 1.41eV, 1.39eV, and

1.35eV have been identified as recombinations involving Ga/As vacancies. Therefore, it is possible that the reason the ratios of the first two peaks to the Cd peak remain constant with additional annealing while the ratio of the 1.35eV peak to the Cd peak increases is that a different lattice atom vacancy is responsible for the first two peaks than for the 1.35eV peak. And the Si₃N₄ cap does not reduce the out-diffusion of Ga and As equally (Ref 9:568, 10:1425).

Cadmium Implanted GaAs with Fluence = 10^{14} ion/cm². The data at a beam energy of 15KV for samples 4 and 4A presented in Table III show the same annealing effects as described for samples 8 and 8A. However, the intensity of the Cd peak after annealing is much greater for sample 8A than for sample 4A. The 15KV electron beam has a maximum penetration in the GaAs crystal of 1.21 μ m. By using equations (3) and (4) the Cd concentration at this depth for samples 8A and 4A is calculated as 8×10^{15} ion/cm³ and 8×10^{17} ion/cm³ respectively. One would expect that the higher Cd ion concentration would give the most intense Cd peak; and yet, the opposite seems to have happened. It is proposed that sample 8A has a greater concentration of Cd ions at the 1.21 μ m depth than sample 4A. The 10^{14} ion/cm² fluence causes a larger damage layer than the 10^{12} ion/cm² fluence, and when these damage layers are annealed a higher density of vacancies is formed in the 10^{14} ion/cm² fluence sample than in the 10^{12} ion/cm² fluence sample. Assuming the rate of diffusion of Cd ions is determined by their interstitial movement and that vacancies

trap the Cd ions then their concentration will be greatest at diffusion depths in the crystal with the lowest fluence implant. This suppressed diffusion effect definitely supports the interstitial substitutional diffusion model (Ref 1:148, 7:162, 23:55).

Cadmium Implanted GaAs with Fluence = 10^{15} ion/cm². The suppression effect is also present for sample 6A. The 15KV beam energy intensity data for sample 6A in Table III shows a marked decrease in intensity of the Cd peak from the 4A and 8A sample Cd peak intensity. The intensity differences are remarkable considering that the Cd ion concentration at the 15KV depth is supposed to be 1000 times greater for sample 6A than for sample 8A. These values cannot be correct, and the interstitial substitutional diffusion model is needed to explain the intensity values. The damage layer data already presented for samples 8, 4, and 6 show the increasing extent of this damage layer with increasing fluence. During annealing this layer provides the vacancies to trap the Cd ions and suppress the diffusion.

V. Conclusions and Recommendations

Conclusions

In this thesis depth-resolved cathodoluminescence was used to study the effects of Cd implantation and annealing in GaAs. Based upon the results and discussion presented in Chapter IV the following conclusions have been reached:

1. Damage layers created by ion implantation can be sharply defined without destruction of the sample by use of the depth-resolved cathodoluminescence experimental technique. This is the most significant conclusion reached. These layers increase in depth as a direct result of increased ion implantation fluence. A 15 minute anneal at temperatures higher than 800°C or an 800°C anneal for longer than 15 minutes is necessary to completely remove the damage layer for those fluences $\geq 10^{14}$ ion/cm².
2. Hot ion implantation produces smaller damage layers than cold ion implantation for the same fluence.
3. LSS theory does not predict the correct concentration of implanted Cd ions in unannealed GaAs at the damage layer boundary for fluences $\geq 10^{14}$ ion/cm².
4. The increasing Cd peak intensity with decreasing fluences found in the annealed samples supports the interstitial substitutional diffusion model.

5. The 1.49eV peak in the implanted samples is a donor-Cd acceptor recombination. This conclusion is based on the study of the Cd peak energy change with temperature.

6. The 1.35eV peak may be caused by strain between the Si_3N_4 cap and the GaAs surface, but further annealing studies are necessary to firmly establish this.

7. The 1.39eV peak is caused by vacancies created by ion implantation and annealing. Peaks at 1.46eV, 1.41eV and 1.35eV are due to vacancies which were native to the 'as grown' GaAs material. These peaks were enhanced through outdiffusion during annealing.

8. The Si_3N_4 cap does not reduce the outdiffusion of Ga and As equally.

Recommendations

Based upon the results of this study the following recommendations are offered:

1. Depth-resolved cathodoluminescence should be used to study ion-implanted epitaxial samples. This would insure that native defects and impurities introduced during growth would be minimized, making the effects of the ion implantation and annealing clearer than in the study just completed.

2. Additional depth-resolved cathodoluminescence data needs to be collected on the change of the damage layer depth with fluence and annealing for Cd-implanted GaAs. Smaller beam energy increments

need to be used to better identify the damage layer boundary. Studies of hot and cold ion implantation with equal fluences should be done to confirm that a hot implant causes less damage than a cold one.

3. Hall effect measurements should be made on annealed ion-implanted GaAs samples that have damage layers which have been studied by depth-resolved cathodoluminescence. This will allow a correlation to be made between electrical activity and damage layer extent as indicated by optical activity.

4. Tellurium implantation should be studied using the depth-resolved cathodoluminescence technique. Since this ion does not diffuse as rapidly as Cd the effects of annealing should be clearer.

5. Annealing effects should be studied further by using longer and hotter anneals than used in this study.

6. The Si_3N_4 cap should be removed from ion-implanted unannealed and annealed samples, and their luminescence compared to that found before cap removal to clearly identify the 1.35eV peak observed in this study.

Bibliography

1. Kazunori, A., et al. "Photoluminescence Study of Cd-Ion Implanted n-GaAs." Japanese Journal of Applied Physics, 15: 145-149 (January 1976).
2. Ashen, D. J., et al. "The Incorporation and Characterization of Acceptors in Epitaxial GaAs." Journal of Physics and Chemistry of Solids, 36: 1041-1053 (1975).
3. Bogardus, E. H. and H. B. Beeb. "Bound Exciton, Band-Acceptor, Donor-Acceptor, and Auger Recombination in GaAs." Physics Review, 176: 993-1002 (December 1968).
4. Boulet, D. L. Depth Resolved Cathodoluminescence of Cadmium Implanted Gallium Arsenide. Unpublished thesis. Wright-Patterson Air Force Base, Ohio: Air Force Institute of Technology, (December 1975).
5. Boyd, G. V. Time-resolved Cathodoluminescence of Cadmium Implanted Gallium Arsenide. Unpublished thesis. Wright-Patterson Air Force Base, Ohio: Air Force Institute of Technology, (June 1976).
6. Bradly, G. S. Materials Handbook. New York: McGraw-Hill, 1971.
7. Casey, H. C., et al. "Dependence of the Diffusion Coefficient on the Fermi Level." Physics Review, 162: 660-668 (October 1967).
8. Chang, L. I., et al. "Vacancy Association of Defects in Annealed GaAs." Applied Physics Letters, 19: 143-145 (September 1971).
9. Chatterjee, P. K., et al. "Photoluminescence from Be-implanted GaAs." Applied Physics Letters, 27: 567-569 (November 1975).
10. _____. "Photoluminescence Study of Native Defects in Annealed GaAs." Solid State Communications, 17: 1421-1424 (December 1975).
11. Chiang, S. Y. and G. L. Pearson. "Photoluminescence Studies of Vacancies and Vacancy-Impurity Complexes in Annealed GaAs." Journal of Luminescence, 10: 313-322 (1975).

12. Cho, A. Y. and I. Hayashi. "Surface Structures and Photoluminescence of Molecular Beam Epitaxial Films of GaAs." Solid State Electronics, 14: 125-132 (1971).
13. Colbaw, K. "Free-to-Bound and Bound-to-Bound Transitions in CdS." Physics Review, 141: 742-749 (January 1966).
14. Cusano, D. A. "Radiative Recombination from GaAs Directly Excited by Electron Beams." Solid State Communications, 2: 353-358 (1964).
15. Dingle, R. "Radiative Lifetimes of Donor-Acceptor Pairs in p-type Gallium Arsenide." Physics Review, 184: 788-796 (August 1969).
16. Fujimoto, M., et al. "Diffusion of Cadmium in Gallium Arsenide." Japanese Journal of Applied Physics, 8: 725-729 (June 1969).
17. Gibbons, J. F. "Ion Implantation in Semiconductors-Part I Range Distribution Theory and Experiments." Proceedings of the IEEE, 56: 295-298 (March 1968).
18. _____, et al. Projected Range Statistics. New York: Halsted Press, 1975.
19. Hanson, W. A. Dose Rate Effects on Radiation Damage of GaAs Using Electroreflectance. Unpublished thesis. Wright-Patterson Air Force Base, Ohio: Air Force Institute of Technology, (March 1976).
20. Hwang, C. J. "Photoluminescence Study of Thermal Conversion in GaAs Grown from Silica Boats." Journal of Applied Physics, 39: 5347-5356 (November 1968).
21. _____. "Evidence for Luminescence Involving Arsenic Vacancy-Acceptor Centers in p-Type GaAs." Physical Review, 180: 827-832 (April 1969).
22. Leite, R. C. C. and A. E. DiGiovanni. "Frequency Shift with Temperature as Evidence for Donor-Acceptor Pair Recombination in Relatively Pure n-Type GaAs." Physical Review, 153: 841-843 (January 1967).
23. Lin, M. S., et al. "Photoluminescence and Electrical Measurements on Manganese Ion-implanted GaAs." Japanese Journal of Applied Physics, 15: 53-56 (January 1976).

24. Llegems, M., et al. "Optical and Electrical Properties of Mn-Doped GaAs Grown by Molecular-Beam Epitaxy." Journal of Applied Physics, 46: 3059-3065 (July 1975).
25. Longini, R. L. "Rapid Zinc Diffusion in Gallium Arsenide." Solid State Electronics, 5: 127-130 (1962).
26. Martinelli, R. U. and C. C. Wang. "Electron-beam Penetration in GaAs." Journal of Applied Physics, 44: 3350-3351 (July 1973).
27. McKelvey, J. P. Solid State and Semiconductor Physics. New York: Harper and Row, 1966.
28. Norris, C. B., et al. "Depth-resolved Cathodoluminescence in Undamaged and Ion-implanted GaAs, ZnS, and CdS." Journal of Applied Physics, 44: 3209-3221 (July 1973).
29. Pierce, B. J. Luminescence and Hall Effect of Ion Implanted Layers in ZnO. Unpublished Dissertation. Wright-Patterson Air Force Base, Ohio: Air Force Institute of Technology, (September 1974).
30. _____ and R. L. Hengehold. "Depth-resolved Cathodoluminescence of Ion-implanted Layers in Zinc Oxide." Journal of Applied Physics, 47: 644-651 (February 1976).
31. Shin, B. K., et al. "Hall-effect Measurements in Cd-implanted GaAs." Journal of Applied Physics, 47: 1574-1579 (April 1976).
32. Sturge, M. D. "Optical Absorption of Gallium Arsenide Between 0.6 and 2.75 eV." Physical Review, 127: 768-773 (August 1962).
33. Willardson, R. K. and A. Beer, editors. Semiconductors and Semimetals. Vol. VIII: Transport and Optical Phenomena. New York: Academic Press, 1966.
34. Williams E. W. and H. B. Bebb. "Photoluminescence in Lightly Doped Epitaxial GaAs: Cd and GaAs: Si." Journal of Physics and Chemistry of Solids, 30: 1289-1293 (September 1968).
35. _____ and D. M. Blacknall. "The Observations of Defects in GaAs Using Photoluminescence at 20°K." Transactions of the Metallurgical Society of AIME, 239: 387-394 (March 1967).

36. Willmann, F., et al. "GaAs Luminescence Transitions to Acceptors in Magnetic Fields." Physica Status Solidi, 60: 751-759 (1973).
37. Woodcock, J. M., et al. "Electrical and Cathodoluminescence Measurements on Ion Implanted Donor Layers in GaAs." Solid State Electronics, 18: 267-275 (1975).

Vita

Joseph Danny Dumoulin was born on 4 June 1947 in Plattsburgh, New York, the son of Joseph N. and Blanche Dumoulin. He attended the State University College of Arts and Sciences at Plattsburgh, Plattsburgh, New York, after graduating from high school in 1964. In 1968 he received the degree of Bachelor of Science in Physics, and he spent the next year teaching Physics, Chemistry, and Mathematics at Mooers Central School, Mooers, New York. Upon completion of Officers Training School in 1969, he received a reserve commission in the United States Air Force. His first assignment was at the National Security Agency, Ft. George G. Meade, Maryland. He was reassigned in 1973 to a Spacetrack site near Diyarbakir, Turkey. In February 1974 he was assigned to the 4000th Aerospace Applications Group, Offutt Air Force Base, Nebraska. Captain Dumoulin began his tour at the Air Force Institute of Technology in June 1975.

Permanent address: 1026 Van Buren Street
Uniondale, New York 11553

UNCLASSIFIED

SECURITY CLASSIFICATION OF THIS PAGE (When Data Entered)

REPORT DOCUMENTATION PAGE		READ INSTRUCTIONS BEFORE COMPLETING FORM
1. REPORT NUMBER GEP/PH/76-2	2. GOVT ACCESSION NO.	3. RECIPIENT'S CATALOG NUMBER
4. TITLE (and Subtitle) DEPTH-RESOLVED CATHODOLUMINESCENCE ON THE EFFECTS OF Cd IMPLANTATION AND ANNEALING IN GALLIUM ARSENIDE		5. TYPE OF REPORT & PERIOD COVERED MS Thesis
7. AUTHOR(s) Joseph D. Dumoulin Captain		6. PERFORMING ORG. REPORT NUMBER
9. PERFORMING ORGANIZATION NAME AND ADDRESS Air Force Institute of Technology (AFIT/EN) Wright-Patterson AFB OH 45433		8. CONTRACT OR GRANT NUMBER(s)
11. CONTROLLING OFFICE NAME AND ADDRESS AFAL/DHR Air Force Avionics Laboratory Wright-Patterson AFB OH 45433		10. PROGRAM ELEMENT, PROJECT, TASK AREA & WORK UNIT NUMBERS 78850613
14. MONITORING AGENCY NAME & ADDRESS (if different from Controlling Office)		12. REPORT DATE December 1976
		13. NUMBER OF PAGES 73
		15. SECURITY CLASS. (of this report) UNCLASSIFIED
		15a. DECLASSIFICATION/DOWNGRADING SCHEDULE
16. DISTRIBUTION STATEMENT (of this Report) Approved for public release; distribution unlimited.		
17. DISTRIBUTION STATEMENT (of the abstract entered in Block 20, if different from Report)		
18. SUPPLEMENTARY NOTES Approved for public release; IAW AFR 190-17 <i>Jerald F. Guess</i> JERALD F. GUESS, Captain, USAF Director of Information		
19. KEY WORDS (Continue on reverse side if necessary and identify by block number) Cathodoluminescence Gallium Arsenide Ion Implantation Annealing		
20. ABSTRACT (Continue on reverse side if necessary and identify by block number) Ten samples of GaAs were examined by depth-resolved cathodoluminescence at temperatures of 10°K and 80°K. Electron beam energies from 1.0KV to 25KV were used. Both cold and hot, 135KV, Cd-implanted GaAs samples with Si ₃ N ₄ caps were studied. A sample of the n-type GaAs substrate was used as a control. Spectra were obtained showing the ion implantation damage layers. The unannealed samples damage layer boundaries were calculated at 0.01 μ m, 0.24 μ m, 0.37 μ m, and 0.61 μ m for fluences of 10 ¹² ion/cm ² , 10 ¹⁴ ion/cm ² , 10 ¹⁵ ion/cm ² , and 10 ¹⁶ ion/cm ² . <i>5g cm 5g cm 5g cm</i>		

DD FORM 1 JAN 73 1473 EDITION OF 1 NOV 65 IS OBSOLETE

* micrometers

UNCLASSIFIED

SECURITY CLASSIFICATION OF THIS PAGE (When Data Entered)

10 to the 12th power

10 to the 14th power

10 to the 15th power

5g cm

UNCLASSIFIED

SECURITY CLASSIFICATION OF THIS PAGE(When Data Entered)

701 = the 14th power
10th 5g cm power

ion/cm² respectively. For fluences $\geq 10^{14}$ ion/cm² an 800°C, 15 minute anneal in flowing argon gas was not sufficient to completely remove the damage layer. An emission peak at 1.488eV changed in energy by only 0.001 eV between 10°K and 80°K, and was assigned to a donor-Cd acceptor recombination. A peak approximately 0.010eV above the band gap energy was observed in many of the implanted samples. Peaks at 1.46eV, 1.41eV, 1.39eV, and 1.35eV increased in intensity upon annealing and were assigned to vacancies, which were enhanced during annealing. The major conclusion reached was that depth-resolved cathodoluminescence was an excellent non-destructive method of sharply defining damage layers produced by ion implantation.

↑

UNCLASSIFIED

SECURITY CLASSIFICATION OF THIS PAGE(When Data Entered)